Supplementary Materials

Introduction

The principal threat to species as a result of human activities is the change in landscapes and resulting habitat loss (Lindenmayer & Fischer, 2013). This is especially important for species with narrow ranges, and therefore more susceptible to minor variations and stochastic events (Manne & Pimm, 2001). As a result of human activities, between 900 and 130,000 species became extinct during the last five centuries (www.iucnredlist.org; Régnier et al., 2015), in connection with human activities, and numerous undescribed species also become extinct every year (Tedesco et al., 2014). These silent extinctions are likely to have a worse impact on biodiversity than estimated as ecological contribution to the environment are poorly known in undescribed species, and virtually unknown for undescribed species (Brodie et al., 2014; e.g., Rix et al., 2017). Indeed, it is not possible to care about what we do not know, and this relationship between taxonomy, knowledge and conservation highlights a need for the urgent taxonomic assessment of all clades). However, conservation effort do generally result in improvements in species conservation statuses, for instance reducing bird extinction rates by 40% (Monroe et al., 2019) and preventing the extinction of dozens of vertebrates in recent times (Bolam et al., 2021). For amphibians as well, conservation activities can result in the decrease of threat, and for instance the Oaxaca Treefrog (*Sarcohyla celata*) was transferred from Critically Endangered to Near Threatened in 2021 following its protection and rigorous habitat management by local communities (Neam & Borzée, 2021).

Clawed salamanders are a peculiar group of lungless salamanders endemic to northeast Asia and a sister lineage to the rest of the family Hynobiidae (Zhang et al., 2006). These salamanders are habitat specialists adapted to life and reproduction in flowing mountain streams or subterranean environments, and their distribution is generally restricted to montane areas of the Russian Far East, northeastern China, the Korean Peninsula and the Japanese Archipelago (Honshu and Shikoku islands; Kuzmin, 1995; Poyarkov et al., 2012). The genus *Onychodactylus* was traditionally considered to contain only two species, *O. japonicus* (Houttuyn) from Japan and *O. fischeri* (Boulenger) from the northeastern Asian mainland (Kuzmin, 1995; Sato, 1943). However, recent phylogenetic and integrative taxonomic studies (Poyarkov et al., 2012; Yoshikawa et al., 2008, 2013; Yoshikawa & Matsui, 2013, 2014, 2022) revealed a previously unknown diversity within *Onychodactylus* and added eight new species to the genus, by describing six new species from Japan (*O. fuscus* Yoshikawa & Matsui, *O. intermedius* Yoshikawa & Matsui, *O. kinneburi* Yoshikawa, Matsui, Tanabe & Okayama, *O. nipponoborealis* Kuro-O, Poyarkov & Vieites, *O. pyrrhonotus* Yoshikawa & Matsui, and *O. tsukubaensis* Yoshikawa & Matsui), two new species from China (*O. zhangyapingi* Che, Poyarkov & Yan, and *O. zhaoermii* Che, Poyarkov & Yan), and one new species from the Korean Peninsula (*O. koreanus* Min, Poyarkov & Vieites). Therefore, there are currently four recognized nominal species of *Onychodactylus* occurring in the mainland Asia: *O. fischeri* (Primorye, Russian Far East), *O. zhangyapingi* (Jilin Province, China), *O. zhaoermii* (Jilin and Liaoning provinces, China and also expected to occur in D.P.R. Korea; Borzée et al., 2021) and *O. koreanus* (Korean Peninsula; Shin et al., 2021b).

The genus *Onychodactylus* is generally declining (Maslova et al., 2018; Suk et al., 2018), and in R. Korea *O. koreanus* was listed as threatened in 1989 under the Protection of Wild Fauna and Flora Act of the Korean Ministry of Environment (as *O. fischeri*). The species was however excluded from the list in 1998 in view of its large population size and large

distributional range, which largely resulted from the identification of *O. koreanus* as *O. fischeri* as the species was not described at that time.

Materials and Methods

Introduction about the species

Within the three *Onychodactylus* clades occurring in R. Korea, haplotypes are not abundantly shared between geographically close populations (Suk et al., 2018), indicating weak gene flow, and weak dispersal abilities of *Onychodactylus*, despite the known migration patterns in fall (Shin et al., 2020b). *Onychodactylus* species are strict ecological specialists (Kuzmin, 1995; Suk et al., 2018) and are generally found in comparatively higher elevation and forested areas near cold mountain streams (Hong, 2017; Kim et al., 2019; Poyarkov et al., 2012). Spawning in the candidate species from Yangsan has not been observed, likely due to the subterranean breeding behaviour typical for *Onychodactylus* species, making it difficult for eggs to be detected (Kuzmin, 1995; Park, 2005).

General sampling

Sampling was conducted in several phases. The first section was conducted in 2002 – 2015 and all voucher specimens, except one from Unmun Mountain (see Poyarkov et al., 2012), were re-used in the present paper for the genetic analysis but not for the morphological comparisons. The collected specimens were stored in 70 % alcohol until 2021, when they were measured for the morphometric analysis. In addition, field surveys were conducted in November and December 2020 for morphological analyses and to collect datapoints for modeling. The surveys were in the form of road cruising in wet evenings in areas where the focal clade was expected to be occurring, on 17, 19, 20 and 27 November, and on 7 and 8 December 2020. For each individual, GPS coordinates were recorded, some adult individuals were measured and released for the taxonomic assessment, but no individual was collected. We also acquired buccal swabs (cotton-tipped swab; 16H22, MedicalWire; Corsham, UK) from three adult individuals, two from Yangsan (35.448333 °N; 128.97055 °E; 340 m a.s.l.) and one from Miryang (35.466442 °N; 128.929128 °E; 280 m a.s.l. (Figure 1); to ascertain the identity of the populations. Specimens collected earlier were subsequently deposited in in the Conservation Genome Resources Bank for Korean Wildlife (CGRB), College of Veterinary Medicine, Seoul National University, R. Korea.

Ethical approval

All applicable international, national, and/or institutional guidelines for the care and use of animals were strictly followed. All animal sample collection protocols complied with the current laws of the Republic of Korea and the People's Republic of China. All observations and experiments conducted in this study are in agreement with the ethical recommendations of the College of Biology and the Environment at Nanjing Forestry University. We did not collect adult individuals as voucher specimen, in line with the IUCN recommendation on research involving species at risk of extinction (IUCN, 1989).

Morphometrics

All individuals included in the morphometric analysis were similarly preserved in 70% alcohol since sampling, and we therefore did not consider shrinking because of dehydration as a problem (Shu et al., 2017). The field identification number of the larvae measured were the following mms1351 to mms1358, mms2585; mms2590 to mm2609; mms3211 to mms3212; mms3616 to mms3621, mms4339; mms5675 to mms5681; mms6683 to mms6684; mms6686 to mms6691. All larvae were estimated to be in their second year of development based on size, and they all had reached the same developmental stage, matching with the stage 28 in other caudata species (Hurney et al., 2015). The individual vouchers

mms2594, mms2599, mms2601 and mms2609 were not included in the analyses. However, the data collected here cannot be compared with live individuals or specimens preserved and stored in other preservatives. A total of 49 larvae were included in the morphometric analysis, such as n = 26 for *O. koreanus* and n = 23 for the candidate species from Yangsan and Miryang. The data were collected with digital callipers (1108–150, Insize; Suzhou, China) to the nearest 0.1 mm, following the methodological recommendations for salamanders in general (Nishikawa et al., 2007) and specifically to the genus (Poyarkov et al., 2012). Each individual was measured three times by the same observer, all samples were measured by the same observer over the course of a single day to ensure accuracy, and the results were averaged for each individual for further analyses. The morphometric variables collected for larval specimens were: SVL—snout-vent-length; TL—tail length; GA—dextral gleno–acetabular distance (minimum distance between axilla and groin measured on the right side of the straightened body); CW—chest width (minimum distance between left and right axillae); FLL—dextral forelimb length (length of the straightened right forelimb measured from axilla to tip of the longest finger of forelimb); HLL—dextral hindlimb length (length of the straightened right hindlimb from groin to tip of the longest toe of hindlimb); HL—head length (from tip of snout to the gular fold at mouth angle); HW—head width (as maximum width of head); EL—dextral eye length (minimum distance from the anterior corner of the right eye to the posterior corner of the right eye); IN—internarial distance; ON—dextral orbitonarial distance (minimum distance between the right external nares and the anterior corner of the eye on the same side of the head); IO—interorbital distance (minimum distance between the upper eyelids) and IC—intercanthal distance (measured as minimum distance between anterior corners of the eyes).

For the subsequent holotype and paratype descriptions, in line with the description of *Onychodactylus koreanus* (Poyarkov et al., 2012), we also recorded OR—orbitorostral distance; 1-FL–4-FL—first to fourth finger lengths; 1-TL–5-TL—first to fifth toe lengths; VTL—vomerine tooth series depth; VTW—vomerine tooth series width; MTH—tail height in the middle of the tail; MTW—tail width in the middle of the tail; MAXTH—maximal tail height; and the following meristic characters CGN —costal grooves number both dextrally and sinistrally (number of costal grooves between the forelimbs and hindlimbs, excluding axillary and inguinal grooves, following Misawa, 1989); VTN—vomerine teeth number in the left and right tooth series; and CGBL—number of costal between adpressed limbs. We also measured these characters for two adults and seven larvae for the species description. The individuals were placed in a 20 % benzocaine bath for 1 min to anesthetize them while acquiring adequate morphological measurements. As we are not aware of any recommended protocol, the individuals were not totally anesthetized, but unable to right themselves for 15 to 20 min and therefore slow enough for adequate morphological measurement. All measurements were conducted on a wet towel at the point of capture, and individuals were released on the spot once alert again.

Supplementary Table S1. Correlation table for all morphological variables for *Onychodactylus sillanus* sp. nov. specimens. We conducted a Pearson's correlation test for all morphological variables included in the analyses (n = 49). Each variable was measured three times and averaged, and data are presented in the form of a ratio with the focal variables divided by SVL

		GA (right)	CW	FFL (right)	HLL (right)	HL	HW	EL (right)	IN	ON (right)	IO	IC
TL	R	-0.577	-0.496	-0.413	0.057	-0.243	-0.424	-0.551	-0.152	0.054	-0.214	-0.458
	p	< 0.001	< 0.001	0.003	0.695	0.093	0.002	< 0.001	0.298	0.712	0.14	0.001
GA (right)	R	-	0.591	0.268	0.021	0.066	0.52	0.34	0.084	-0.115	0.155	0.178
	p	-	< 0.001	0.062	0.886	0.65	< 0.001	0.017	0.567	0.433	0.288	0.222
CW	R	-	-	0.328	-0.022	0.209	0.726	0.261	0.014	-0.201	0.198	0.132
	p	-	-	0.021	0.88	0.149	< 0.001	0.071	0.924	0.165	0.172	0.367
FFL (right)	R	-	-	-	0.506	0.148	0.208	0.058	0.226	0.035	0.338	0.193
	p	-	-	-	< 0.001	0.31	0.152	0.691	0.118	0.813	0.018	0.185
HLL (right)	R	-	-	-	-	0.112	-0.141	-0.272	0.172	-0.143	0.094	-0.054
	p	-	-	-	-	0.443	0.335	0.058	0.237	0.328	0.52	0.715
HL	R	-	-	-	-	-	0.281	0.22	0.427	0.198	0.354	0.573
	p	-	-	-	-	-	0.051	0.128	0.002	0.173	0.012	< 0.001
HW	R	-	-	-	-	-	-	0.317	0.108	0.012	0.201	0.239
	p	-	-	-	-	-	-	0.027	0.462	0.932	0.165	0.098
EL (right)	R	-	-	-	-	-	-	-	0.154	-0.117	-0.003	0.304
	p	-	-	-	-	-	-	-	0.29	0.422	0.983	0.034
IN	R	-	-	-	-	-	-	-	-	0.193	0.466	0.259
	p	-	-	-	-	-	-	-	-	0.183	0.001	0.073
ON (right)	R	-	-	-	-	-	-	-	-	-	-0.025	0.037
	p	-	-	-	-	-	-	-	-	-	0.866	0.802
IO	R	-	-	-	-	-	-	-	-	-	-	0.312
	p	-	-	-	-	-	-	-	-	-	-	0.029

Following established protocols (Borzée & Min, 2021) and in line with the general literature on morphological analyses (Hayek et al., 2001; Lleonart et al., 2000), we used a ratio to correct for body size in relation with individual growth. To calculate the ratio, we divided each variable by the SVL value of the same individual. To harness as much of the variation possible expressed by the 12 morphological measurements collected for the 49 individuals, and because 20 measurements were correlated (Pearson correlation; Supplementary Table S1), we opted for a factor reduction analysis. We selected a principal component analysis (PCA) and tested the resulting principal components (PCs) for significant difference between the two clades. Factor extraction for the PCA was conducted under a varimax rotation with Kaiser normalisation. The rotations converged in six iterations and variables were selected as loading into a PC if > 0.50, ensuring that each variable loaded into one of the PCs (Supplementary Table S2). Once the PCs were extracted, we tested for significant differences between the two clades using a one-way ANOVA with PCs as dependent variables and clades as independent variables.

Supplementary Table S2. Component matrix with the loading factors of each variable into the PCs. The factors were extracted with a principal component analysis under a varimax rotation with Kaiser normalisation. Rotations converged in 6 iterations. The representative PCs are in bold. The value used as the cut-off was 0.47, and loading variables are in bold. The PCs were selected if the eigenvalues were >1, based on varimax rotations. The total loading cumulative percentage is in bold. Each PC explained between 8.45 and 30.73% of variation, and PC3 was significantly different between the two clades.

		PC1	PC2	PC3	PC4
Rotated Component					
Tail length	**-0.64**	-0.39	0.03	0.38	
Gleno-acetabular distance	**0.79**	0.05	0.08	-0.18	
Chest width	**0.88**	0.01	0.11	-0.05	
Forelimb length (right)	0.36	0.25	**0.71**	-0.06	
Hindlimb length (right)	-0.12	0.04	**0.87**	-0.10	
Head length	0.12	**0.79**	0.01	0.11	
Head width	**0.85**	0.15	-0.09	0.15	
Eye length (right)	0.37	0.36	-0.42	**-0.50**	
Internarial distance	-0.01	**0.70**	0.23	0.19	
Orbitonarial distance (right)	-0.04	0.25	-0.19	**0.79**	
Interorbital distance	0.16	**0.57**	0.35	0.09	
Intercanthal distance	0.13	**0.76**	-0.13	-0.25	
Variance					
Eigenvalues	3.69	1.93	1.57	1.01	
% of Variance	30.73	16.11	13.07	8.45	
ANOVA					
Mean square	0.25	0.39	7.52	0.06	
df	47,48	47,48	47,48	47,48	
F	0.25	0.39	8.74	0.06	
p	0.621	0.536	**0.005**	0.816	

In addition, we performed a visual comparison of the shape and number of vomerine teeth between the candidate species from Yangsan and Miryang and the two most closely phylogenetically related *Onychodactylus* species: *O. koreanus* and *O. zhaoermii*, based on the graphical representation from Poyarkov et al. (2012). We did not conduct any statistical analysis regarding the number of vomerine teeth due to the low sample size (n = 3) for the candidate species.

Phylogenetics

The phylogenetic analysis was conducted using the samples already reported in Poyarkov et al. (2012) and Suk et al. (2018) for the three mitochondrial DNA markers, including cytochrome *b* (Cyt *b*), 1st subunit of cytochrome oxidase *c* (*COI*), and a partial sequence of 16S rRNA fragment. We also added the four newly collected samples (two from Yangsan, one from Unmun mountain, and one from Miryang), thus ascertaining the genetic assignment of the population in Miryang, and the monophyly with the samples from Yangsan. The DNA was extracted from the buccal swabs using the DNeasy Blood and Tissue kit (Qiagen, Hilden, Germany) following the manufacturer's protocol. Details on the PCR reactions followed Poyarkov et al. (2012), with the same primers and PCR conditions for 16S rRNA and *COI* as reported by Poyarkov et al. (2012); for amplification of Cyt *b* gene fragment we used the primers Onycho_Cytb_up70F (forward: 5′-CATAGCAAGTAAAGCTAAATAAATCAT-3′; Yoshikawa et al., 2008) and salamander_Cytb_RN2 (reverse: 5′-YTYTCAATCTTKGGYTTACAAGACC-3′; Matsui et al., 2008). Quality check and trimming of sequences were conducted using Geneious Prime 2019.1.3 (https://www.genei ous.com).

Nucleotide sequences were initially aligned in MAFFT v.6 (Katoh et al., 2002) with default parameters, and then checked by eye and slightly adjusted in BioEdit v.7.0.5.2 (Hall, 1999). Genetic distances and sequence statistics were calculated using MEGA-X (Kumar et al., 2018) and DnaSP v. 5 (Librado & Rozas, 2009). We deposited the resulting sequences in GenBank (accession numbers MZ404936; MZ404937 and MZ404938 Supplementary Table 3). We added GenBank data for all other ten currently recognized *Onychodactylus* species, a candidate species from Gangwon, Korea (*Onychodactylus* sp. A), as well as seven species of hynobiid salamanders (*Hynobius chinensis*, *H. arisanensis*, *Pachyhynobius shangchengensis*, *Ranodon sibiricus*, *Batrachuperus yenyuanensis*, *Paradactylodon persicus and Salamandrella keyserlingii*; Supplementary Table 3) which were used as outgroups (following the phylogenetic results of Chen et al., 2015; Weisrock et al., 2013; Zheng et al., 2011, 2012). Altogether, the final alignment included sequences from 79 hynobiid representatives, including six specimens of *O. zhaoermii*, 40 specimens of *O. koreanus*, one specimen of *Onychodactylus* sp. A from Gangwon, and 16 specimens of the candidate *Onychodactylus* species from Yangsan and Miryang (Supplementary Table 3).

We concatenated the sequence data of 16S rRNA, *COI* and Cyt *b* for a final alignment of 2357 bp. The best fit substitution models were determined with PartitionFinder v. 2.1.1 (Lanfear et al., 2017), using the Akaike Information Criterion and the Bayesian Information Criterion for the Maximum Likelihood (ML) and Bayesian Inference (BI) analyses, respectively. The 16S rRNA gene fragment was treated as a single partition, whereas Cyt *b* and *COI* were partitioned by codon position. For ML and BI analyses, the best partitioning scheme and models of nucleotide substitutions were: 16S rRNA (GTR+I+G), 1st position of Cyt *b* (TrN), 2nd position of Cyt *b* (HKY+I), 3rd position of Cyt *b* (HKY), 1st position of *COI* (SYM+I), 2nd position of *COI* (F81+I), and 3rd position of *COI* (HKY+G).

Supplementary Table S3. Sequences and voucher specimens of *Onychodactylus* and outgroup hynobiid taxa used in this study.

No.	Sample ID	Species	Region	Locality	Cyt b	16S rRNA	COI
1	JQ710885	*Hynobius chinensis*	China	Hubei	JQ710885	JQ710885	JQ710885
2	EF462213	*Hynobius arisanensis*		Taiwan, Alishan	EF462213	EF462213	EF462213
3	MK890366	*Pachyhynobius shangchengensis*	China	Henan	MK890366	MK890366	MK890366
4	AJ419960	*Ranodon sibiricus*	China	Xinjiang	AJ419960	AJ419960	AJ419960
5	DQ333818	*Batrachuperus yenyuanensis*	China	Sichuan	DQ333818	DQ333818	DQ333818
6	MK737945	*Paradactylodon persicus*	Iran	Gorgan	MK737945	MK737945	MK737945
7	JX508762	*Salamandrella keyserlingii*	China	Heilongjiang	JX508762	JX508762	JX508762
8	NP-OF2-1	*Onychodactylus fischeri*	Russia	Primorskiy Krai, Tigrovoy	JX157971	JX158086	JX158208
9	KJ627181	*Onychodactylus zhangyapingi*	China	Jilin, Linjiang	KJ627181	KJ627181	KJ627181
10	MKO-2-1	*Onychodactylus nipponoborealis*	Japan	Aomori, Hirosaki	JX158074	JX158197	JX158320
11	NPH-109-1	*Onychodactylus japonicus*	Japan	Kanagawa, Hakone	JX158050	JX158171	JX158293
12	KI-17	*Onychodactylus kinneburi*	Japan	Ehime, Ishizuchi-san	JX158283	JX158284	JX158285
13	OJ112	*Onychodactylus pyrrhonotus*	Japan	Kyoto, Nantan-shi	AB452922	—	—
14	OJ50	*Onychodactylus tsukubaensis*	Japan	Ibaraki, Tsukuba-san	AB452860	—	—
15	KUHE48284	*Onychodactylus fuscus*	Japan	Fukushima, Tadami	AB923989	—	—
16	KUHE47455	*Onychodactylus intermedius*	Japan	Fukushima, Koriyama	AB924003	—	—
17	KJ627182	*Onychodactylus zhaoermii*	China	Changbai-Shan	KJ627182	KJ627182	KJ627182
18	KIZ-YPX10504	*Onychodactylus zhaoermii*	China	Changbai-Shan	JX158235	JX157998	JX158116
19	KIZ-YPX10505	*Onychodactylus zhaoermii*	China	Liaoning, Qinchengzi	JX158236	JX157999	JX158117
20	KIZ-YPX10506	*Onychodactylus zhaoermii*	China	Liaoning, Qinchengzi	JX158237	JX158000	JX158118
21	CBS-2010-18	*Onychodactylus zhaoermii*	China	Liaoning, Kuandian	JX158234	JX157997	JX158114
22	CBS-2010-19	*Onychodactylus zhaoermii*	China	Liaoning, Kuandian	—	—	JX158115
23	PDS A-1	*Onychodactylus koreanus*	Korea	North Chungcheong, Naeam-myeon	JX158261	JX158024	JX158143
24	PDS A-2	*Onychodactylus koreanus*	Korea	North Chungcheong, Naeam-myeon	JX158262	JX158025	JX158142
25	PDS A-3	*Onychodactylus koreanus*	Korea	North Chungcheong, Naeam-myeon	JX158263	JX158026	JX158144
26	PDS A-4	*Onychodactylus koreanus*	Korea	North Chungcheong, Naeam-myeon	JX158264	JX158027	JX158141
27	PDS A-5	*Onychodactylus koreanus*	Korea	North Chungcheong, Naeam-myeon	JX158265	JX158028	JX158145

28	PDS B-1	*Onychodactylus koreanus*	Korea	Gangwon, Nae-myeon	JX158247	JX158010	JX158132
29	PDS B-2	*Onychodactylus koreanus*	Korea	Gangwon, Nae-myeon	JX158248	JX158011	JX158131
30	PDS B-3	*Onychodactylus koreanus*	Korea	Gangwon, Nae-myeon	JX158249	JX158012	JX158130
31	PDS B-4	*Onychodactylus koreanus*	Korea	Gangwon, Nae-myeon	JX158250	JX158013	JX158129
32	PDS B-5	*Onychodactylus koreanus*	Korea	Gangwon, Nae-myeon	JX158251	JX158014	JX158128
33	PDS C-1	*Onychodactylus koreanus*	Korea	Gangwon, Seo-myeon	JX158238	JX158001	JX158120
34	PDS C-2	*Onychodactylus koreanus*	Korea	Gangwon, Seo-myeon	JX158239	JX158002	JX158119
35	PDS C-3	*Onychodactylus koreanus*	Korea	Gangwon, Seo-myeon	JX158240	JX158003	JX158121
36	PDS C-4	*Onychodactylus koreanus*	Korea	Gangwon, Seo-myeon	JX158241	JX158004	JX158122
37	PDS D-1	*Onychodactylus koreanus*	Korea	Gangwon, Dongnae-myeon	JX158242	JX158005	JX158123
38	PDS D-2	*Onychodactylus koreanus*	Korea	Gangwon, Dongnae-myeon	JX158243	JX158006	JX158126
39	PDS D-3	*Onychodactylus koreanus*	Korea	Gangwon, Dongnae-myeon	JX158244	JX158007	JX158124
40	PDS D-4	*Onychodactylus koreanus*	Korea	Gangwon, Dongnae-myeon	JX158245	JX158008	JX158125
41	IK20	*Onychodactylus koreanus*	Korea	North Jeolla, Naejangsan NP	JX158272	JX158033	JX158155
42	H059	*Onychodactylus koreanus*	Korea	North Jeolla, Naejangsan NP	JX158273	JX158034	JX158156
43	H095	*Onychodactylus koreanus*	Korea	Gangwon, Chiaksan NP, Gillaji	JX158252	JX158015	JX158133
44	H096	*Onychodactylus koreanus*	Korea	Gangwon, Chiaksan NP, Gillaji	JX158253	JX158016	—
45	MMS-258	*Onychodactylus koreanus*	Korea	Gangwon, Singi-myeon	JX158259	JX158022	JX158139
46	MMS-259	*Onychodactylus koreanus*	Korea	Gangwon, Singi-myeon	JX158260	JX158023	JX158140
47	MMS-141	*Onychodactylus koreanus*	Korea	Gangwon, Chiaksan NP, Chiak-san	JX158254	JX158017	JX158134
48	MMS-142	*Onychodactylus koreanus*	Korea	Gangwon, Chiaksan NP, Chiak-san	JX158246	JX158009	JX158127
49	H031	*Onychodactylus koreanus*	Korea	South Gyeongsang, Jirisan NP	JX158275	JX158035	JX158157
50	H032	*Onychodactylus koreanus*	Korea	South Gyeongsang, Jirisan NP	JX158276	JX158036	JX158158
51	H082	*Onychodactylus koreanus*	Korea	South Gyeongsang, Jirisan NP	JX158277	JX158037	JX158160
52	IK71	*Onychodactylus koreanus*	Korea	North Jeolla, Naedong	JX158271	JX158031	—
53	IK70	*Onychodactylus koreanus*	Korea	North Jeolla, Naedong	JX158270	JX158032	JX158154
54	H083	*Onychodactylus koreanus*	Korea	South Gyeongsang, Jirisan NP	JX158278	JX158038	JX158161
55	H084	*Onychodactylus koreanus*	Korea	South Gyeongsang, Jirisan NP	JX158279	JX158039	JX158159
56	MMS-109	*Onychodactylus koreanus*	Korea	South Gyeongsang, Jirisan NP	JX158280	JX158040	JX158162

57	MMS-104	*Onychodactylus koreanus*	Korea	Gangwon, Bongpyeong-myeon	JX158255	JX158018	JX158135
58	MMS-105	*Onychodactylus koreanus*	Korea	Gangwon, Bongpyeong-myeon	JX158256	JX158019	JX158136
59	MMS-242	*Onychodactylus koreanus*	Korea	Gangwon, Seokbyeong-san	JX158257	JX158020	JX158137
60	MMS-243	*Onychodactylus koreanus*	Korea	Gangwon, Seokbyeong-san	JX158258	JX158021	JX158138
61	MMS-244	*Onychodactylus koreanus*	Korea	North Jeolla, Jucheon-Myeon	JX158268	JX158029	JX158153
62	MMS-245	*Onychodactylus koreanus*	Korea	North Jeolla, Jucheon-Myeon	JX158269	JX158030	JX158152
63	MMS1753	*Onychodactylus* sp. A	Korea	Gangwon, Yangyang-gun	KX590686	—	—
64	MMS-257	*Onychodactylus sillanus* sp. nov.	Korea	South Gyeongsang, Yangsan-si, Dong-myeon	JX158281	JX158041	JX158163
65	MMS-444	*Onychodactylus sillanus* sp. nov.	Korea	South Gyeongsang, Yangsan-si, Dong-myeon	JX158282	JX158042	JX158164
66	MMS 7270 / NAP-05131	*Onychodactylus sillanus* sp. nov.	Korea	North Gyeongsang, Unmunsan	OL771443	OL830810	OL792790
67	MMS10917	*Onychodactylus sillanus* sp. nov.	Korea	South Gyeongsang, Yangsan-si, Dong-myeon	MZ404936	—	—
68	MMS10918	*Onychodactylus sillanus* sp. nov.	Korea	South Gyeongsang, Yangsan-si, Dong-myeon	MZ404937	—	—
69	MMS10919	*Onychodactylus sillanus* sp. nov.	Korea	South Gyeongsang, Myriang-si	MZ404938	—	—
70	MMS443	*Onychodactylus sillanus* sp. nov.	Korea	South Gyeongsang, Yangsan-si	KX590671	—	—
71	MMS1350	*Onychodactylus sillanus* sp. nov.	Korea	South Gyeongsang, Yangsan-si	KX590672	—	—
72	MMS1333	*Onychodactylus sillanus* sp. nov.	Korea	South Gyeongsang, Yangsan-si	KX590673	—	—
73	MMS1334	*Onychodactylus sillanus* sp. nov.	Korea	South Gyeongsang, Yangsan-si	KX590674	—	—
74	MMS1335	*Onychodactylus sillanus* sp. nov.	Korea	South Gyeongsang, Yangsan-si	KX590675	—	—
75	MMS1331	*Onychodactylus sillanus* sp. nov.	Korea	South Gyeongsang, Yangsan-si	KX590676	—	—
76	MMS1343	*Onychodactylus sillanus* sp. nov.	Korea	South Gyeongsang, Yangsan-si	KX590677	—	—
77	MMS1349	*Onychodactylus sillanus* sp. nov.	Korea	South Gyeongsang, Yangsan-si	KX590678	—	—
78	MMS1344	*Onychodactylus sillanus* sp. nov.	Korea	South Gyeongsang, Yangsan-si	KX590679	—	—
79	MMS1339	*Onychodactylus sillanus* sp. nov.	Korea	South Gyeongsang, Yangsan-si	KX590680	—	—

We conducted the ML analysis in the IQ-TREE webserver (http://iqtree.cibiv.univie.ac.at/). We employed 1,000 bootstrap pseudoreplicates via the ultrafast bootstrap (UFBS; Hoang et al., 2018) approximation algorithm, and nodes having ML UFBS values of 95 and above were a-priori considered highly supported, while the nodes with values of 90–94 were considered well-supported, and the nodes with values of 70–89 were considered as tendencies. BI trees were generated using MrBayes v. 3.1.2 (Ronquist & Huelsenbeck, 2003). The BI analyses were performed using three heated and one cold Metropolis Coupled Markov Chain Monte Carlo chains for 200 million generations, with sampling every 100 generations. We checked the convergence of the runs and that the effective sample sizes were all above 200 by exploring the likelihood plots using TRACER v. 1.6 (Rambaut & Drummond, 2013). The initial 10% of trees were discarded as burn-in. After burn-in, trees of two independent runs were combined in a single majority consensus topology. Confidence in BI tree topology was assessed using the posterior probability (BI PP; Huelsenbeck & Ronquist, 2001). We a priori considered BI PP 0.95 or greater as significant support (Leaché & Reeder, 2002). For divergence time estimates within *Onychodactylus* we relied on the earlier results by Suk et al. (2018).

Ecological niche modeling

We implemented ecological niche models (ENMs) to provide additional evidence of divergence between *O. koreanus* and the candidate species from extreme south-eastern R. Korea (Pyron & Burbrink, 2009; Rissler & Apodaca, 2007). To generate ENMs, we first collected georeferenced occurrence points for *O. koreanus* and the candidate species from our own survey data, the Global Biodiversity Information Facility (GBIF; accessed 7 October 2020; https://doi.org/10.15468/dl.khx67d), VertNet (searched under *O. fischeri*; accessed 22 September 2020), voucher specimens deposited in the Ewha Woman's University Natural History Museum (Shin et al., 2020a), and from the survey dataset of the National Institute of Ecology accessed through the EcoBank platform (Kim et al., 2021). In total, we collected 921 occurrence points for *O. koreanus* and 28 occurrence points for the candidate species (Figure 1). Species assignment was based on the results of the genetic analyses. For environmental variables, we used 19 bioclimatic and elevation layers downloaded from WorldClim 2.1 (https://www.worldclim.org; Fick & Hijmans, 2017), slope, coniferous, broadleaf and mixed forest layers downloaded from EarthEnv (https://www.earthenv.org; Amatulli et al., 2018; Tuanmu & Jetz, 2014), and Euclidean distance to water bodies derived from the elevation layer in ArcMap 10.8.1 (ESRI, Redlands, CA). All environmental layers were in 1-km spatial resolution. The same general data collection methodology and resulting occurrence dataset for *O. koreanus* are also provided in Shin et al. (2021b).

Our methods for selecting environmental variables broadly follow Rissler & Apodaca (2007). To select non-collinear environmental variables, we first sampled 50,000 random points across the Korean Peninsula using the *dismo* package (Hijmans et al., 2021) in R version 3.6.3 (R Core Team, 2020). Next, we extracted environmental raster values from these random points and conducted a Spearman's test in the R package *ntbox* (Osorio-Olvera et al., 2020). Excluding highly correlated (coefficient > 0.7) variables, our environmental layers were reduced to the following: annual mean temperature (bio1), mean diurnal range (bio2), isothermality (bio3), annual precipitation (bio12), precipitation of wettest months (bio13), precipitation seasonality (bio15), broadleaf forest cover, needleleaf forest cover, mixed forest cover, slope, and distance to nearest water bodies. Next, we spatially thinned our occurrence dataset to reduce spatial clustering of occurrence points. Using the *spThin* package in R (Aiello-Lammens et al., 2015) and applying a 1-km thinning distance parameter, we retained 187 unique occurrence points for *O. koreanus* and seven unique occurrence

points for the candidate species. This thinning resulted in the points used for the analysis to be at least 1 km away from each other.

Using the reduced sets of environmental and occurrence data, we implemented ENMs separately for *O. koreanus* and the candidate species in the software Maxent (version 3.4.1; https://biodiversityinformatics.amnh.org/open_source/maxent). We used Maxent because of the algorithm's ability to explicitly account for the spatial bias of species occurrence points (via a "bias file"; Shin et al., 2021a). Another benefit of Maxent is that the algorithm can be implemented with small sample size (Pearson et al., 2007). While the number of independent datapoints for the candidate species is small (n = 7), a previous study has demonstrated predictive ability of Maxent models when implemented with sample size greater than $n \geq 5$ (Pearson et al., 2007).

For *O. koreanus*, we specifically tuned the Maxent model parameters using the R package *ENMeval* (Muscarella et al., 2014). Furthermore, using a published dataset used to generate ENMs of *O. koreanus* (Shin et al., 2021b; http://dx.doi.org/10.17632/yc3nw4d9f2.2), we employed target group background sampling to correct for spatial bias of *O. koreanus* occurrence points between R. Korea and the Democratic People's Republic of Korea (hereafter D.P.R. Korea). From 48 candidate models run in *ENMeval*, we selected model parameters with the Hinge feature and a regularization multiplier of 2 based on the AICc value (Muscarella et al., 2014). In addition to these settings, we enabled random seed, sampled 10,000 target group background points, set maximum iteration to 500, used 30% of data for model testing, and applied Maximum Training Sensitivity plus Specificity threshold rule (Shin et al., 2021b). Using these parameters, the ENM for *O. koreanus* was calibrated on the entire extent of mainland Korean Peninsula (see Shin et al., 2021b for justification of modelling extent).

For the candidate species we implemented Maxent using random seed, auto features, a default regularization multiplier (= 1), 10,000 random background points sampled within a 20-km radius buffer around each occurrence point, testing data percentage of 20, and maximum iterations of 500, and applied Minimum Training Presence threshold rule. To generate the ENM for the candidate species we first calibrated the model on the environmental layers clipped by a 20-km circular buffer around each occurrence point. This model was then projected across the entire extent of mainland Korean Peninsula.

For both clades, we run 10 bootstrap replicates of the ENMs, and we averaged the results of 10 replicate runs for downstream analyses. We evaluated model performance using the area under the Receiver Operating Characteristic curve (AUC), True Skill Statistic (TSS; Allouche et al., 2006), and the plotted distribution. Regarding the ENM for the candidate species we implemented an additional model validation with a jackknife test as described in Pearson et al. (2007) due to the small sample size used for model construction.

Niche differentiation

We implemented two tests to investigate niche differentiation between *O. koreanus* and the candidate species. First, we examined whether the ENMs generated for each clade were identical using niche identity test. We run 100 Maxent replicates using the same set of occurrences and the environmental dataset used for niche modeling. We used Schoener's *D* and *I* statistics to summarize the test results.

Next, we conducted the ribboning analysis as described in Glor & Warren (2011). This analysis tests for the presence of unsuitable habitat separating two suitable regions. The mountains inhabited by each *O. koreanus* and the candidate species are separated by a low elevation plain called the Yangsan Fault unsuitable for the species (Kyung, 2010), with a known impact on phylogeographic structures (Bae & Suk, 2015). Thus we considered the ribboning analysis to be most appropriate to test niche differentiation between the two

Onychodactylus among the three types of range breaking analyses introduced in Glor & Warren (2011). To implement the ribboning analysis, we first defined the region of unsuitable habitat ("ribbon") between the ranges of *O. koreanus* and the candidate species by joining five outermost occurrence points of *O. koreanus* and two outermost occurrence points of the candidate species in a minimum convex polygon (MCP). Next, we sampled 97 random points (half the number of *O. koreanus* and the candidate species occurrences combined) within this MCP, representing a third "clade" inhabiting a zone of habitat unsuitable to both *Onychodactylus* clades. Therefore, we generated separate ENMs for *O. koreanus*, the candidate species, and the "ribbon clade" in 100 Maxent replicates and used Schoener's *D* and *I* statistics to summarize the test results. Both niche identity and ribboning tests were implemented using the R package *ENMTools* (Warren et al., 2021).

Climate change

As with other members of the genus *Onychodactylus*, the candidate species is likely prone to anthropogenic climate change (Borzée et al., 2019a; Kuzmin, 1995; Shin et al., 2021b; Suk et al., 2018). Thus, we projected the ENM of current habitat suitability to two representative concentration pathways (RCPs) corresponding to intermediate (RCP 4.5) and extreme (RCP 8.5) climate change scenarios for the years 2050 and 2070. Following a previous study, we selected the CCSM4 climate model under the Coupled Model Intercomparison Project Phase 5 (CMIP5) downloaded from WorldClim 2.1 (Borzée et al., 2019a; Shin et al., 2021b). For model projections, only the bioclimatic variables were changed according to each RCP and time frame, and topographic and vegetation layers remained constant for the lack of corresponding climate change scenarios for these variables. Using the projected output models and the corresponding minimum training presence threshold values, we also calculated the total area of suitable habitat under each climate change scenario. We conducted model projections and area calculations within the 20-km circular buffer surrounding all known occurrence points of the candidate species.

Conservation assessment

We conducted a threat assessment following the IUCN Red List categories and criteria due their robustness (Maes et al., 2015) and the representation of threats at the global scale (Mace et al., 2008). The IUCN Red List classifies species into three threatened categories: Vulnerable, Endangered or Critically Endangered. Evaluations are conducted against quantitative thresholds for five criteria that determine whether a species is at risk of extinction: A, population size reduction; B, geographic range size; C, small population size and decline; D, very small population and/or restricted distribution; and E, quantitative analysis of extinction risk. A species can be assessed for any or all of the five criteria simultaneously and if it does not meet one of these criteria it is placed into one of the non-threatened IUCN categories (Least Concern and Near Threatened). Here, we follow the IUCN Red List categories and criteria (IUCN Species Survival Commission, 2012) to suggest an assessment for the candidate *Onychodactylus* species.

All threats, habitats, uses and trades are presented following the IUCN Red List criteria and categories (www.iucnredlist.org/resources/redlistguidelines), and in the order specified. The focal clade here is impacted by residential and commercial developments in parts of its range (similarly to *Hynobius yangi*; Borzée & Min, 2021), but it is not known to be used or traded. The clade is found along cold forested streams with high humidity and dense leaf litter (Hong, 2017). In addition, the clade is also under generalized threats such as habitat degradation and climate change resulting in the warming and deoxygenation of waters at the country level (Borzée, 2020; Jane et al., 2021), a critical set of variables for salamanders (Borzée et al., 2019a; Mahler & Bourgeais, 2013; Zhang et al., 2020). Global warming was called to be

limited to a 1.5 °C increase above preindustrial levels by the Paris Climate Agreements (Cop21, 2015), a difficult but insufficient request (Mundaca et al., 2019) under which the environment is still expected to be severely impacted, and especially water resources (IPCC, 2014, 2018). Even if the targets specified by the Paris Climate Agreements are reached, air temperature in northeast Asia is still expected to increase by 2.7 °C (peaking at 7.0 °C under a 4 °C scenario if the Paris Climate Agreements are not held; Xu et al., 2017), and humidity by 3.3% (13% under a 4 °C scenario; Xu et al., 2017).

- Population size reduction (category A)

The population size reduction is measured over the longer of 10 years or 3 generations, here 21 to 27 years based on the development time of the genus (Lee & Park, 2016), and a longevity expected to be around 17 years for a closely related species (Smirina, 1994). When the number of individuals is not known, the population reduction can be projected through a decline in area of occupancy (AOO), extent of occurrence (EOO) and/or habitat quality (Category A3(c)), here we used the values provided by the projection for the impact of climate change on the habitat.

- Geographic range (category B)

The geographic range is expressed in terms of AOO or EOO, and here we rely on the EOO as we do not have data for the AOO. First, we converted the continuous probability map from the Maxent output model into a binary presence/absence map. For this purpose, we used the model calibrated on the buffered extent to prevent the inclusion of suitable area outside the known range of the candidate species. We used the Minimum Training Presence threshold calculated in Maxent as the cut-off for binary conversion. Next, we generated a minimum convex polygon (MCP) connecting all known occurrence points of the candidate species (n = 27) and calculated the area of MCP using the R package *ConR* (Dauby, 2020).

- Categories C, D and E

The criteria for small population size and decline, very small or restricted populations and quantitative analyses rely on knowing the number of individuals. However, this information is not available for this candidate species and these categories cannot be used in this study.

Results

Morphometrics

The morphometric analyses demonstrated significant differences between *Onychodactylus koreanus* and the candidate *Onychodactylus* species from Yangsan and Miryang (Supplementary Figure S1; Supplementary Table S4). The visual comparison of the vomerine teeth showed that the candidate species is more similar to *O. zhaoermii* in shape but the number of teeth is similar to *O. koreanus*, noting the small sample size used for comparisons (Supplementary Figure S2).

Phylogenetic relationships

Onychodactylus fischeri from the Russian Far East was suggested as the sister lineage to all remaining species of *Onychodactylus* with strong support (98/1.0, hereafter node support values are given for ML UFBS/BI PP, respectively; Figure 1). Within the latter group, all lineages of *Onychodactylus* from Japan (including *O. japonicus*, *O. nipponoborealis*, *O. tsukubaensis*, *O. fuscus*, *O. intermedius*, *O. kinneburi* and *O. pyrrhonotus*) grouped into a significantly supported monophylum (93/0.91; Figure 1). The remaining mainland populations of *Onychodactylus,* at the exception of *O. fischeri* and *O. zhangyapingi* from Jilin Province of northeast China, formed a strongly supported clade hereafter referred to as *O. koreanus* species group (98/0.97; Figure 1). The phylogenetic position of *O. zhangyapingi* is poorly supported, as this species showed a tendency to group

with the Japanese *Onychodactylus* clade, though with insignificant support; a similar topology was also reported by Poyarkov et al. (2012).

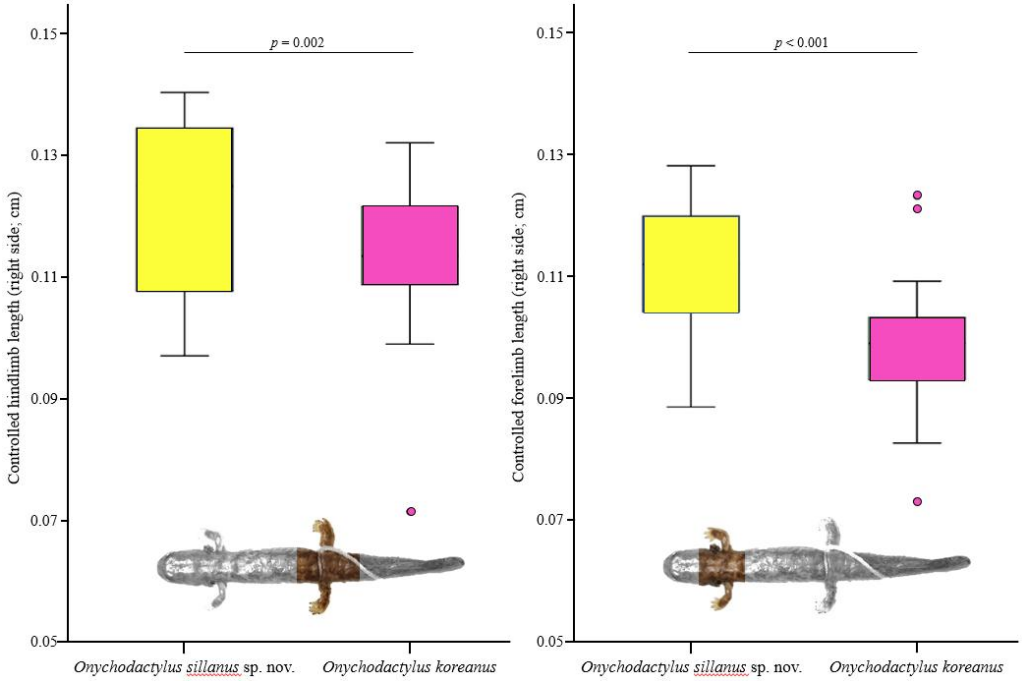

Supplementary Figure S1. Morphometric comparison of limb length between *Onychodactylus koreanus* and *Onychodactylus sillanus* sp. nov. PC3 was the only significantly different PC between the two clades, represented by the length of front- and hindlimbs. Both front- and hindlimbs are significantly longer in *Onychodactylus sillanus* sp. nov. than in *O. koreanus*.

Supplementary Table S4. Descriptive statistics for morphological variables measured on larvae of *Onychodactylus koreanus* and *Onychodactylus sillanus* sp. nov**.** The data is not controlled for SVL as used for the analyses.

	Onychodactylus sillanus sp. nov.				*Onychodactylus koreanus*			
	mean	SD	min	max	mean	SD	min	max
SVL	38.48	3.84	31.68	45.04	35.65	4.23	27.49	40.86
TL	33.02	4.07	26.18	39.98	31.51	5.96	18.88	39.24
GA (right)	19.57	2.23	14.68	23.01	18.33	2.46	12.87	22.57
CW	5.71	0.96	3.79	7.19	5.57	0.71	4.34	7.26
FFL (right)	7.97	1.32	5.48	9.96	6.55	0.92	5.18	8.02
HLL (right)	8.74	1.58	6.43	11.04	7.59	1.33	4.02	9.44
HL	8.19	1.11	6.10	10.32	8.04	0.79	5.47	9.17
HW	7.38	0.86	5.85	8.50	6.99	0.89	5.32	9.16
EL (right)	2.51	0.33	1.87	3.13	2.38	0.25	1.91	3.06
IN	3.56	0.43	2.36	4.30	3.20	0.53	2.12	4.45
ON(right)	1.55	0.24	1.15	2.09	1.35	0.41	0.63	2.26
IO	2.16	0.43	1.17	2.84	1.93	0.34	1.20	2.42
IC	4.16	0.35	3.67	4.87	3.84	0.47	3.02	4.51

Within the *O. koreanus* species group our analyses revealed four well-supported clades (100/1.0) of putatively species-level differentiation in agreement with the earlier

results of Suk et al. (2018). The *O. zhaoermii* populations from Liaoning in northeast China were suggested as a sister lineage to all remaining members of *O. koreanus* species group inhabiting the Korean Peninsula (95/0.91).

The uncorrected genetic *p*-distance calculated from the Cyt *b* gene fragment between the candidate *Onychodactylus* species from Yangsan and Miryang and other congeners varied from p = 13.74 (with *O. fischeri*) to p = 6.49 (with *O. koreanus*) and p = 6.59 (with *Onychodactylus* sp. A from Gangwon; see Supplementary Table S5). The divergence time between these lineages was estimated by Suk et al. (2018) as ca. 6.82 mya (5.38 – 8.20). Despite the presence of several well-supported subclades within *O. koreanus,* the overall topological relationship remains unresolved (Figure 1).

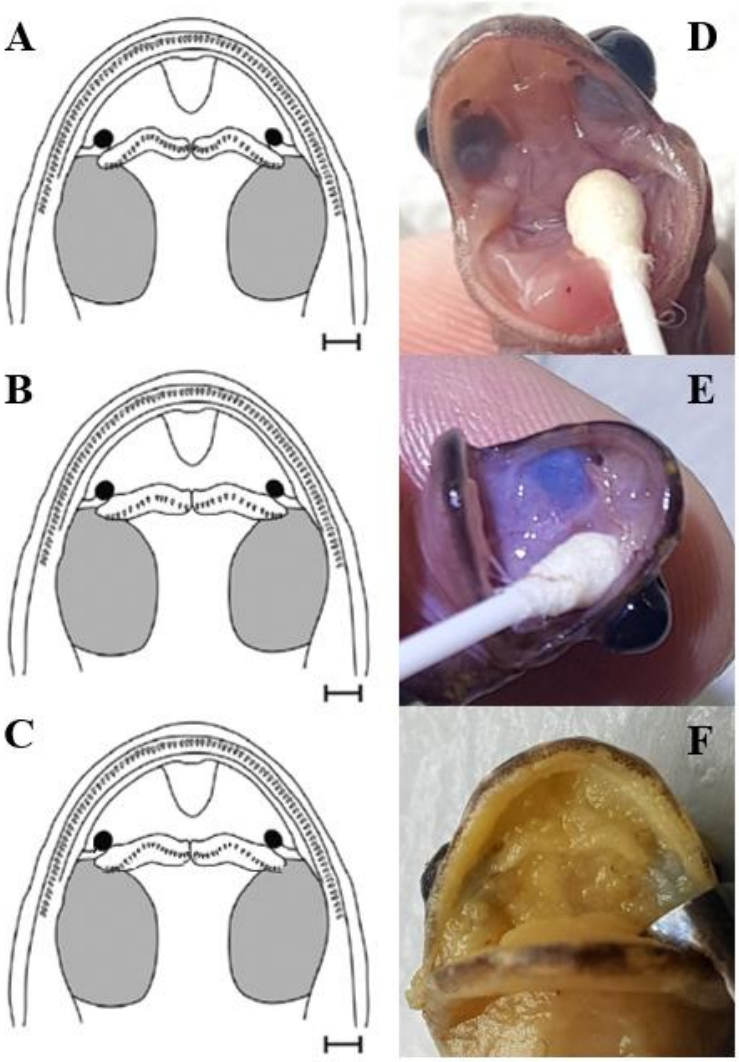

Supplementary Figure S2. Schematic drawing and details of vomeral teeth in palatal view of open mouth. The shape of the vomeral tooth row in *Onychodactylus sillanus* sp. nov. is similar to *O. zhaoermii* but number of teeth is similar to *O. koreanus* (noting that n = 3 for *O. sillanus* sp. nov.). (A) *Onychodactylus koreanus* from Poyarkov et al., 2012. (B) *Onychodactylus zhaoermii* from Poyarkov et al., 2012. (C) *Onychodactylus sillanus* sp. nov., the head shape is modified from Poyarkov et al., 2012 for graphic consistency. (D+E) *Onychodactylus sillanus* sp. nov. pictures when swabbing. (F) Holotype *Onychodactylus sillanus* sp. nov.

Supplementary Table S5. Uncorrected *p*-distance (percentage) between the sequences of Cyt *b* mtDNA gene (below the diagonal), and intraspecific genetic *p*-distance (above the diagonal) of *Onychodactylus* species included in phylogenetic analyses.

	Species	**1**	**2**	**3**	**4**	**5**	**6**	**7**	**8**	**9**	**10**	**11**	**12**	**13**
1	*O. fischeri*	—	0.91	1.01	0.98	1.01	0.98	1.07	1.00	1.06	0.90	0.82	0.94	0.87
2	*O. zhangyapingi*	15.20	—	0.83	0.78	0.84	0.87	0.83	0.89	0.89	0.91	0.89	0.94	0.81
3	*O. nipponoborealis*	14.41	9.05	—	0.70	0.78	0.81	0.69	0.75	0.74	0.85	0.78	0.90	0.85
4	*O. japonicus*	14.59	9.05	6.15	—	0.69	0.75	0.73	0.74	0.72	0.86	0.77	0.86	0.84
5	*O. kinneburi*	14.67	8.96	7.56	6.77	—	0.64	0.73	0.84	0.77	0.86	0.81	0.95	0.86
6	*O. pyrrhonotus*	14.24	10.90	8.26	8.26	5.27	—	0.88	0.86	0.83	0.91	0.79	0.90	0.88
7	*O. tsukubaensis*	14.50	9.05	6.41	6.85	7.91	8.96	—	0.62	0.72	0.77	0.76	0.84	0.74
8	*O. intermedius*	14.94	10.28	7.12	8.35	8.70	9.49	5.54	—	0.60	0.91	0.85	0.96	0.85
9	*O. fuscus*	14.76	9.75	6.59	7.12	7.38	8.96	5.45	4.22	—	0.82	0.87	0.93	0.84
10	*O. zhaoermii*	15.01	11.60	9.30	10.44	9.83	10.79	9.83	11.06	10.44	**0.21**	0.75	0.74	0.79
11	*O. koreanus*	14.48	12.32	9.16	10.67	10.47	10.93	9.89	11.38	10.62	8.63	**1.94**	0.66	0.64
12	*Onychodactylus* sp. A	14.85	11.25	9.67	10.81	10.98	11.60	10.46	11.60	10.98	8.80	7.65	—	0.69
13	*O. sillanus* sp. nov.	13.74	10.19	8.53	9.24	9.39	9.74	8.75	10.34	10.10	6.96	6.49	6.59	**0.17**

Ecological niche modeling

In the ENM of *O. koreanus*, slope had the highest contribution, followed by annual mean temperature (bio1), annual precipitation (bio12), mixed forest cover, needleleaf forest cover, precipitation of wettest months (bio13), distance to nearest water bodies, broadleaf forest cover, mean diurnal range (bio2), isothermality (bio3), and precipitation seasonality (bio15; Supplementary Table S6). In contrast, the ENM for the candidate species showed that the mean diurnal range (bio2) had the highest contribution, followed by needleleaf forest cover, slope, distance to nearest water bodies, mixed forest cover, broadleaf forest cover, annual precipitation (bio12), annual mean temperature (bio1), isothermality (bio3), precipitation seasonality (bio15), and precipitation of wettest months (bio13; Supplementary Table S6).

Supplementary Table S6. Contribution of environmental variables used to generate ecological niche models of *Onychodactylus koreanus* and *Onychodactylus sillanus* sp. nov. The contribution of each variable to niche models is considerably different between species. The asterisks indicate variables with highest contribution in each species.

Variables	**Contribution (%)**	
	Onychodactylus koreanus	*Onychodactylus sillanus* **sp. nov.**
Annual mean temperature (bio1)	24.2	1.4
Mean diurnal range (bio2)	0.2	35.0*
Isothermality (bio3)	0.1	1.0
Annual precipitation (bio12)	7.8	3.2
Precipitation of wettest months (bio13)	2.1	0
Precipitation seasonality (bio15)	0.1	0.3
Broadleaf forest cover	0.6	3.7
Needleleaf forest cover	5	31.5
Mixed forest cover	5.8	5.1
Slope	53.3*	12.5
Distance to nearest water bodies	0.8	6.2

The ENMs for both species were also congruent with the known occurrence points. The predicted habitat suitability of *O. koreanus* largely followed the main mountain ranges and associated mountain chains in R. Korea and extends northward into central D.P.R. Korea. On the other hand, the predicted area of high suitability for the candidate species was mostly restricted to the area around Yangsan and Miryang (Supplementary Figure S3). When projected across the Korean Peninsula, the ENM for the candidate species predicted additional areas of intermediate to high habitat suitability (0.4 ~ 1.0) on the southwestern and eastern coasts of R. Korea, as well as on the northeastern and western coasts of D.P.R. Korea (Supplementary Figure S3).

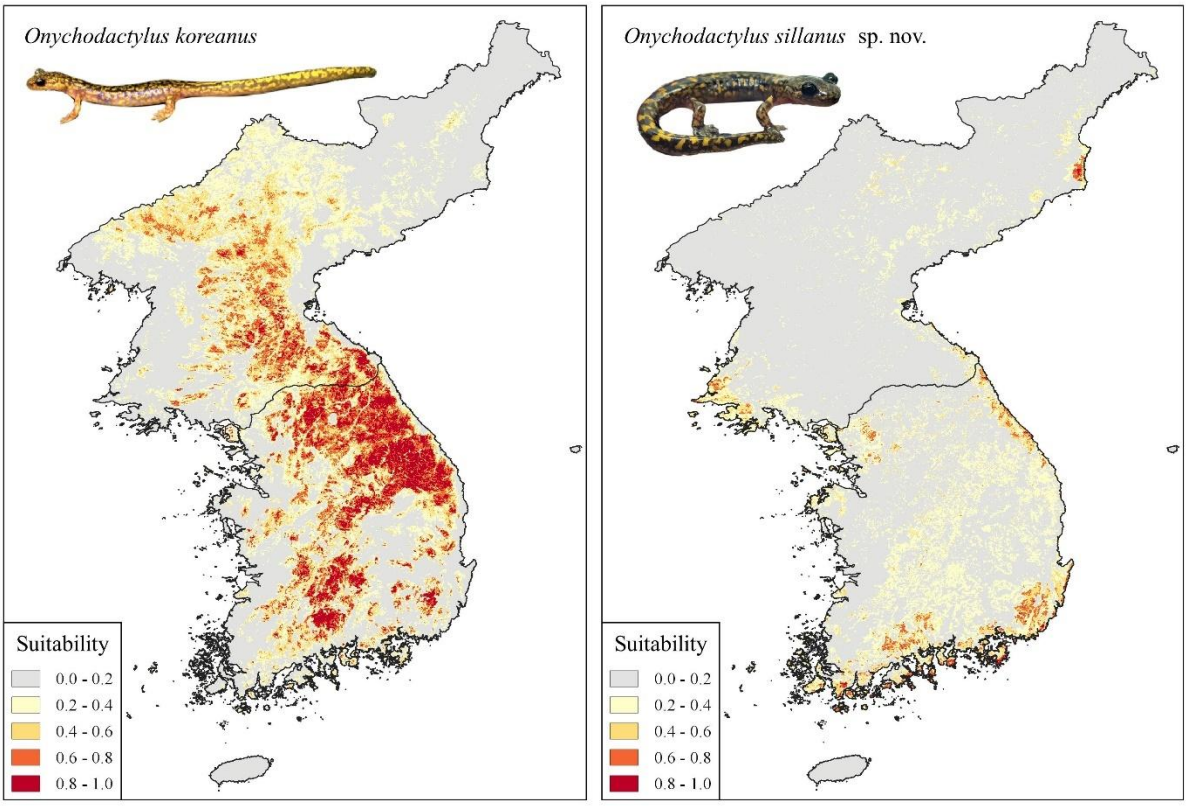

Supplementary Figure S3. Comparison of Maxent habitat suitability models between *Onychodactylus koreanus* and *Onychodactylus sillanus* sp. nov. Note the significant differences in predicted habitat suitability between the two species across the Korean Peninsula. While some overlap of predicted habitat suitability can be found, the actual known ranges of *O. koreanus* and *Onychodactylus sillanus* sp. nov. do not overlap.

Genus *Onychodactylus* Tschudi, 1838

***Onychodactylus sillanus* sp. nov. Min, Borzée & Poyarkov**

This is the supplementary data to the publication http://zoobank.org/urn:lsid:zoobank.org:act:C62AAA19-197A-4B6C-BA6C-AD231FDA0874 where the species is officially described.

Three specimens were designated as paratypes, including CGRB15898 (field ID MMS6688; Supplementary Figure S4)

Measurements and counts of the type series. Measurements and counts of the type series are presented in Supplementary Table S4 & S7.

Supplementary Figure S4. *Onychodactylus sillanus* sp. nov**.** paratype (CGRB15898; Yangsan; 35.306°N, 129.074°E) in preservative. (A) General dorsal view of the paratype; (B) general ventral view of the paratype. SVL = 82.67 mm. Note the presence of black keratinous claws specific to the species.

Supplementary Table S7. Measurements (in mm) and counts of the type series of *Onychodactylus sillanus* sp. nov. For character abbreviations see Materials and Methods.

Specimen ID	CGN(L)	CGN(R)	VTN(L)	VTN(R)	SVL	TL	GA	IC
CGRB15897	11	11	21	22	54.8	51.8	26.5	6.5
CGRB15906	11	11	18	19	51.0	53.2	27.0	5.7
CGRB 15907	12	12	20	20	54.8	56.9	27.9	5.7
Specimen ID	**CW**	**CGBL**	**MAXTH**	**MTH**	**MTW**	**1-FL**	**2-FL**	**VTW**
CGRB15897	6.3	-1	7.1	4.7	4.0	1.6	2.2	4.5
CGRB15906	7.6	-1	-	5.1	4.6	1.7	2.0	-
CGRB 15907	7.5	-1	4.3	4.3	3.8	1.8	2.5	4.6

Specimen ID	HLL	HL	HW	EL	IN	ON	IO	IC	OR
CGRB15897	15.0	12.0	8.5	3.4	5.0	2.7	3.2	6.5	5.2
CGRB15906	14.5	12.3	8.0	3.0	4.7	2.1	3.0	5.7	3.9
CGRB 15907	18.5	14.3	8.6	3.8	5.0	2.0	2.7	5.7	4.5
Specimen ID	**4-FL**	**1-TL**	**2-TL**	**3-TL**	**4-TL**	**5-TL**	**VTL**	**VTW**	
CGRB15897	2.0	1.6	2.1	3.1	3.0	2.7	1.9	4.5	
CGRB15906	1.9	1.5	2.0	3.0	2.8	2.6	-	-	
CGRB 15907	2.1	1.9	2.6	3.7	3.3	2.1	1.9	4.6	

Additional measurements for the holotype CGRB15897 include (all in mm): OR: 5.2; 1-FL: 1.6; 2-FL: 2.2; 3-FL: 3.3; 4-FL: 2.0; 1-TL: 1.6; 2-TL: 2.1; 3-TL: 3.1; 4-TL: 3.0; 5-TL: 2.7; VTL: 1.9; VTW: 4.5; MTH: 4.7; MTW: 4.0; MAXTH: 7.1. Additional counts for the holotype CGRB15897 include: CGN(L): 11; CGN(R): 11; CGBL: -1; VTN(L): 21; VTN(R): 22. Additional measurements (all in mm) and counts for CGRB15906 (field ID MMS-7207) include: OR: 3.9; 1-FL: 1.7; 2-FL: 2.0; 3-FL: 2.6; 4-FL: 1.9; 1-TL: 1.5; 2-TL: 2.0; 3-TL: 3.0; 4-TL: 2.8; 5-TL: 2.6; MTH: 5.1; MTW: 4.6; MAXTH: 5.1; CGN(L): 11; CGN(R): 11; CGBL: -1; VTN(L): 18; VTN(R): 19. Additional measurements (all in mm) and counts for CGRB 15907 (field ID MMS 7270 / NAP-05131) OR: 4.5; 1-FL: 1.8; 2-FL: 2.5; 3-FL: 3.1; 4-FL: 2.1; 1-TL: 1.9; 2-TL: 2.6; 3-TL: 3.7; 4-TL: 3.3; 5-TL: 2.1; VTL: 1.9; VTW: 4.6; MTH: 4.3; MTW: 3.8; MAXTH: 4.3. Additional counts include: CGN(L): 12; CGN(R): 12; CGBL: -1; VTN(L): 20; VTN(R): 20.

Additional morphological measurements of referred specimens. We also measured the characters given in Supplementary Table S4 for two adults (one male and one female), and six juveniles (larvae), collected from Miryang, Republic of Korea (35.4489°N, 128.9708 °E; 110 m a.s.l.), which were subsequently released upon taking the measurements. Male (in mm): SVL: 82.18, TL: 102.3, GA right: 41.5, CW: 9.2, FFL right: 17.0, FFL left: 17.2, HLL right: 22.8, HLL left: 22.3, HL: 15.2, HW: 12.3, EL right: 5.3, EL left: 5.4, IN: 6.7, ON right: 3.3, ON left: 3.7, IO: 4.4, OR right: 5.8, OR left: 6.1, IC: 7.9, CGN right: 11, CGN left: 11. Female (in mm): SVL: 75.29, TL: 89.7, GA right: 36.9, CW: 7.6, FFL right: 15.9, FFL left: 15.4, HLL right: 17.0, HLL left: 16.7, HL: 14.3, HW: 11.4, EL right: 4.7, EL left: 4.6, IN: 5.8, ON right: 2.7, ON left: 2.8, IO: 4.0, OR right: 5.3, OR left: 4.6, IC: 6.0, CGN right: 11, CGN left: 11. Juveniles (n = 6; mean ± SD): SVL: 89.3 ± 8.04, TL: 41.91 ± 3.78, GA right: 18.53 ± 9.25, CW: 5.51 ± 0.57; FFL right: 12.02 ± 1.39, FFL left: 11.93 ± 1.33, HLL right: 13.06 ± 1.99, HLL left: 13.12 ± 1.86, HL: 11.52 ± 0.64, HW: 8.43 ± 0.52, EL right: 3.54 ± 0.18, EL left: 3.68 ± 0.2, IN: 4.58 ± 0.43, ON right: 2.13 ± 0.36, ON left: 2.12 ± 0.4, IO: 3.11 ± 0.2, OR right: 4.2 ± 0.7, OR left: 3.88 ± 0.68, IC: 4.96 ± 0.17, CGN right (median): 11 ± 1, CGN left (median): 11 ± 1.

Description of the holotype (Supplementary Figure S5). A subadult specimen (presumably, female) fully metamorphosed, in a poor state of preservation (toes on right hindlimb decayed

and almost absent; ca. 1 cm of the tail tip damaged; forelimbs partially dehydrated), fixed and preserved in 75% ethanol, with a SVL of 54.8 mm (measured on the preserved specimen; Supplementary Figure S5).

Head flattened, comparatively long and narrow, much longer than wide (HL/HW ratio 1.41), head noticeably wider than neck (Supplementary Figure S5C). Tongue large, elliptical, distinctly widening towards its anterior free end. Snout long (OR/HL ratio 0.43); snout rounded in lateral view (Supplementary Figure S5E), obtusely rounded in dorsal view (Supplementary Figure S5C). Nostrils small, with dorsolateral orientation, not protuberant, widely spaced and distant from snout tip (IN/HL ratio 0.42). Eyes protuberant in dorsal and lateral views (Supplementary Figure S5C, E), eye diameter shorter than snout length and the internarial distance (EL/OR ratio 0.65; EL/IN ratio 0.68). Orbits close to each other, interorbital distance short (IO/HL ratio 0.26; EL/IC ratio 0.52). Eyelids present, well-developed; labial folds absent; gular fold distinct. Parotoid glands absent. Distinct longitudinal postorbital groove running from the posterior corner of eye towards the angle of the mouth; postorbital groove almost the same length as the eye; a distinct transverse groove running upwards from the mouth angle to join the postorbital groove, approximately two times shorter than latter. A distinct longitudinal groove running posteriorly of the mouth angle, separating the parotoid area from the swollen elongated subparotoidal protuberance, and further continuing to the gular fold. The subparotoidal protuberance distinct, elongated, oval-shaped, swollen. Vomerine teeth in two transverse notably bended shallow arch-shaped series, forming a «^^»-shaped figure (Supplementary Figure S5H); the medial ends of the inner branches of the left and right vomerine tooth series contacting each other; 21 vomerine teeth in the left vomerine tooth series and 20 vomerine teeth in the right series; the inner branches slightly curving anteriorly; the outer branches notably longer than the inner branches; their lateral ends located more posteriorly than the ends of the inner branches (Supplementary Figure S5H).

Body elongated, cylindrical and slender; chest rather narrow (CW/SVL ratio 0.12). The skin on dorsum and venter smooth. A middorsal groove well-developed, extending from the base of tail to the base of the head. Eleven costal grooves present both on the right and left sides of the body. Cloaca as a short, elongated slit.

Limbs slender, hindlimbs slightly longer and more robust than the forelimbs; when forelimb and hind limb are adpressed towards each other against the flank, the digit tips do not meet; a distinct gap more than 1 costal segment present between toes and fingers of the adpressed limbs; FLL/GA ratio 0.53; HLL/GA ratio 0.57. Palmar or tarsal tubercles on palms or feet absent. Four fingers and five toes lacking digital webbing; in order of decreasing length, the relative lengths of the fingers: F1 < F4 < F2 < F3; relative length of toes: T1 < T2 < T5 < T4 < T3. Tips of fingers and toes rounded, black cornified claws present on all fingers (Supplementary Figure S5F, G), not discernible on toes (since the hindlimbs are partially decayed). Hindlimbs with a fleshy skinfold running along the posterior edge of the hindlimb. Tail short and its tip partially damaged (TL/SVL ratio 1.54). Tail cylindrical in transverse section at the anterior third of its length; turning to laterally compressed at the middle of its length. Caudal fin absent. Tail tip slightly tapered.

Coloration of the holotype (Supplementary Figure S5). Coloration of the holotype in life unknown; after seven years in preservative dorsum dark-brown with light beige or yellowish spots on the dorsal surfaces of head, trunk, limbs and tail (Supplementary Figure S5A). Ventrally uniform light greyish-brown with indistinct greyish mottling on chest and trunk and tail flanks (Supplementary Figure S5B). The principal pattern of the original coloration does not change and is clearly recognizable.

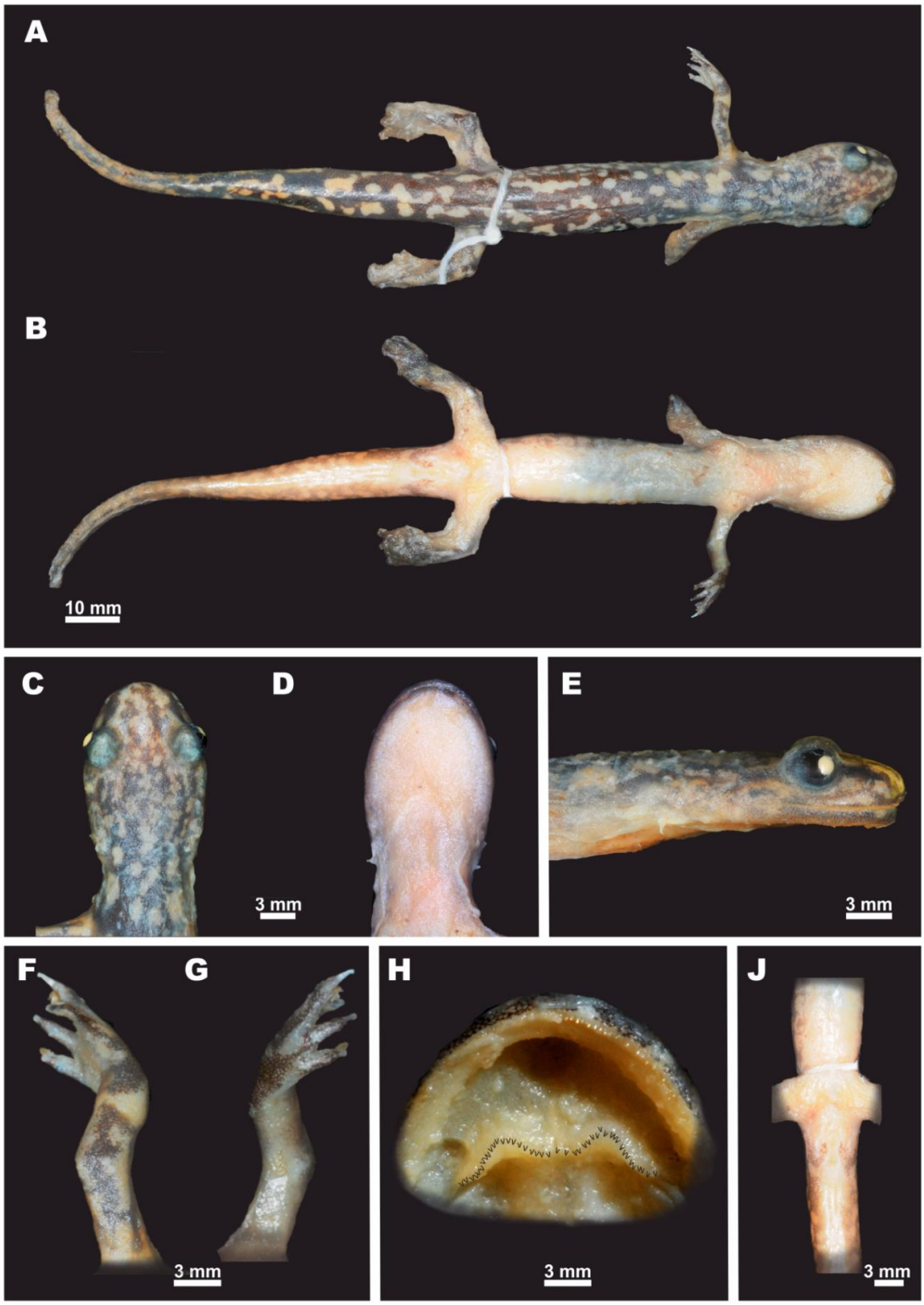

Supplementary Figure S5. Holotype of *Onychodactylus sillanus* sp. nov. (CGRB15897, subadult) from South Gyeongsang Province, Yangsan-si, Dong-myeon, Republic of Korea, in preservative. A: Dorsal view; B: Ventral view; C: Head, dorsal view; D: Head, ventral view; E: Head, lateral view; F: Opisthenar view of left hand; G: Volar view of left hand; H: Palatal region showing the vomerine tooth series; J: Ventral view of cloacal area. Photos by Nikolay A. Poyarkov.

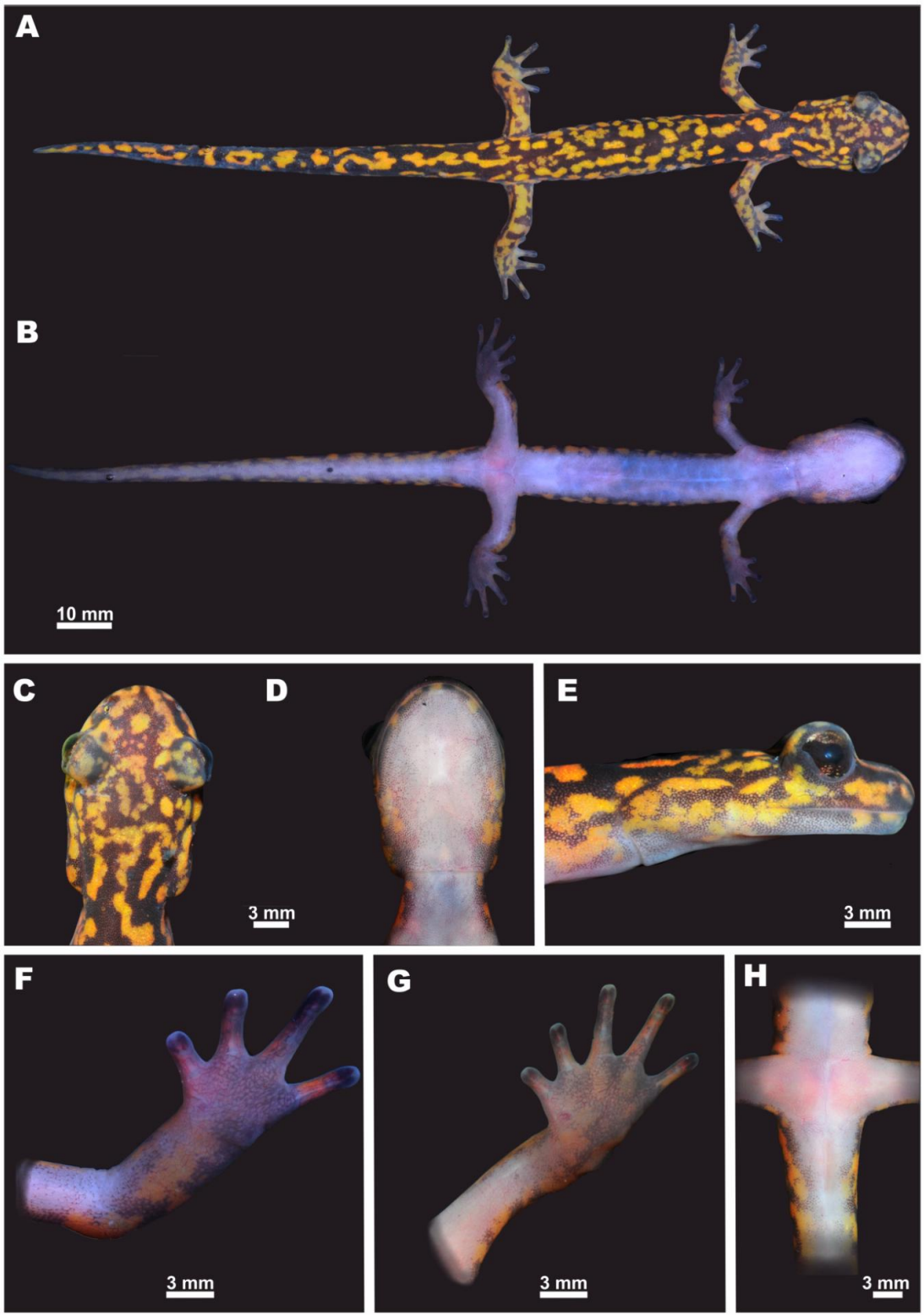

Supplementary Figure S6. Paratype of *Onychodactylus sillanus* sp. nov. (CGRB 15907, subadult) from North Gyeongsang Province, Unmun Mountain, Republic of Korea, in life. A: Dorsal view; B: Ventral view; C: Head, dorsal view; D: Head, ventral view; E: Head, lateral view; F: Volar view of left hand; G: Plantar view of left foot; H: Ventral view of cloacal area. Photos by Nikolay A. Poyarkov.

Variations (Supplementary Figures S1 – S2 & S6 – S7). The paratypes resemble the holotype very closely in all aspects of coloration and pattern. Meristic and mensural variations are presented in Supplementary Table S7. Specimen CGRB 15907 is in a good state of preservation and has the following life coloration (Supplementary Figure S6). Dorsum dark slate-black, varying to dark-lavender-brown at the flanks of body and tail (Supplementary Figure S6A). Flanks of tail and body distinctly lighter than dorsum, dark lavender-gray. Costal grooves darker than costal segments. Head laterally reddish-brown turning lavender-gray ventrally (Supplementary Figure S6E). Ventral surfaces bright violet-grey or lavender-grey (Supplementary Figure S6B). Ventral surfaces of the belly slightly translucent. Limbs dorsally dark reddish-brown, ventrally lavender gray to dark gray. Dorsal sides of the body, head and tail covered with numerous bright-orange to golden elongated spots, forming a denser reticulated pattern on dorsal surfaces of head, getting more longitudinally elongated at mid-trunk and further to the dorsal surfaces of the tail. Light markings vary in size. On body and head flanks the light spots become less intense in coloration; they merge with the light ventral coloration along the belly margins; light markings absent on the ventral side of the body, tail or head. Iris brownish with dark copper speckles dorsally and ventrally (Supplementary Figure S6E). The pupil is horizontal and oval shaped.

Natural history. Biology of the new species is poorly studied. As in other *Onychodactylus* species, *O. sillanus* sp. nov. occurs in moist, cool and shady places in evergreen and mixed montane forests in the mountains of Yangsan and Miryang in the south-eastern region of the Korean Peninsula, where it was recorded from 83 to 871 m a.s.l. (299.3 ± 179; Mean ± SD). The new species inhabits clean, fast-running streams in mountain areas, in association with pine trees or deciduous forests. Adults were recorded in the upstream on elevation from 280 to 800 m a.s.l.; whereas larvae and metamorphs were observed also in lower elevations (Figure 1 and Supplementary Figure S7) hiding under stones or tree-logs in the streambed.

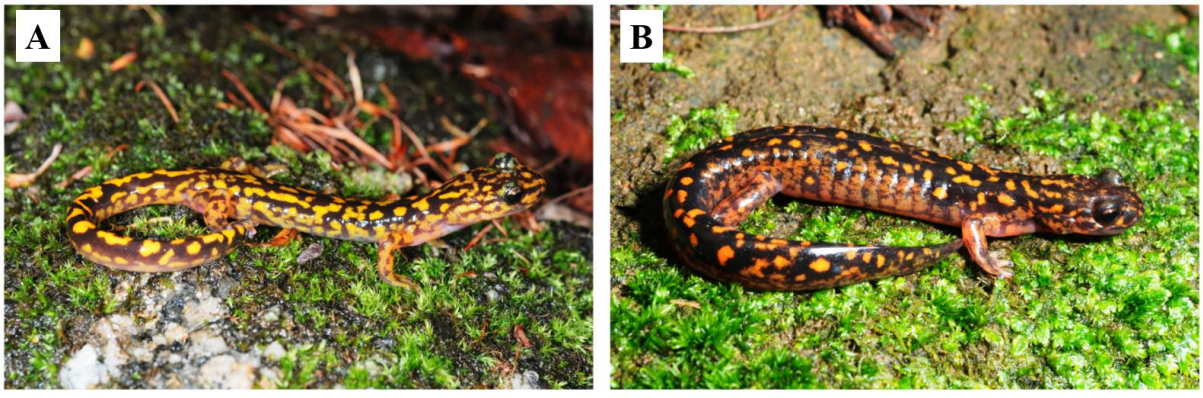

Supplementary Figure S7. *Onychodactylus sillanus* sp. nov. in life. A: adult male from North Gyeongsang Province, Yangsan-si, Republic of Korea, in life (not collected); B: subadult paratype (CGRB 15907) from North Gyeongsang Province, Unmun Mountain, Republic of Korea, in life. A: metamorph from North Gyeongsang Province, Yangsan-si, Dong-myeon, Republic of Korea, in life (not collected); B: larva from North Gyeongsang Province, Yangsan-si, Dong-myeon, Republic of Korea, in life (not collected),

Adults and juveniles were found at night, active on large rock boulders on a steam bed, always in proximity of water. The species seems to favour wet warm night of very late autumn to disperse along streams, or on roads on rainy days. Larvae can be found during both

daytime and night time, throughout most of the year, at the exception of the coldest months. In Yangsan area, *O. sillanus* sp. nov. is found in sympatry with *Hynobius yangi*, *Glandirana emeljanovi* and *Rana uenoi*, with larvae potentially feeding on other amphibian larvae and freshwater invertebrates. Like in other species of *Onychodactylus*, breeding in the new species most likely takes place in streams or slow-moving subterranean water bodies; however, the details of its reproductive biology remain unknown.

Current distribution and climate change. The models for 2070 predicted 24.4 km^2 of suitable habitat under the RCP 4.5 and 37.6 km^2 of suitable habitat under the RCP 8.5 (Figure 1). Under the RCP 4.5 scenario, these reductions in suitable habitat translate into 87.6% (MCP) and a 95.9% (Maxent binary) reduction by 2050, and 90.5% (MCP) and 96.9% (Maxent binary) reduction by 2070. Under the RCP 8.5 scenario, the reductions reach 91.6% (MCP) and 97.3% (Maxent binary) by 2050 and 85.5% (MCP) and 95.3% (Maxent binary) by 2070.Modelling placed the EOO of *O. sillanus* sp. nov. at 792.7 km^2 based on the Maxent binary map and 258.3 km^2 based on the MCP (Supplementary Figure S8).

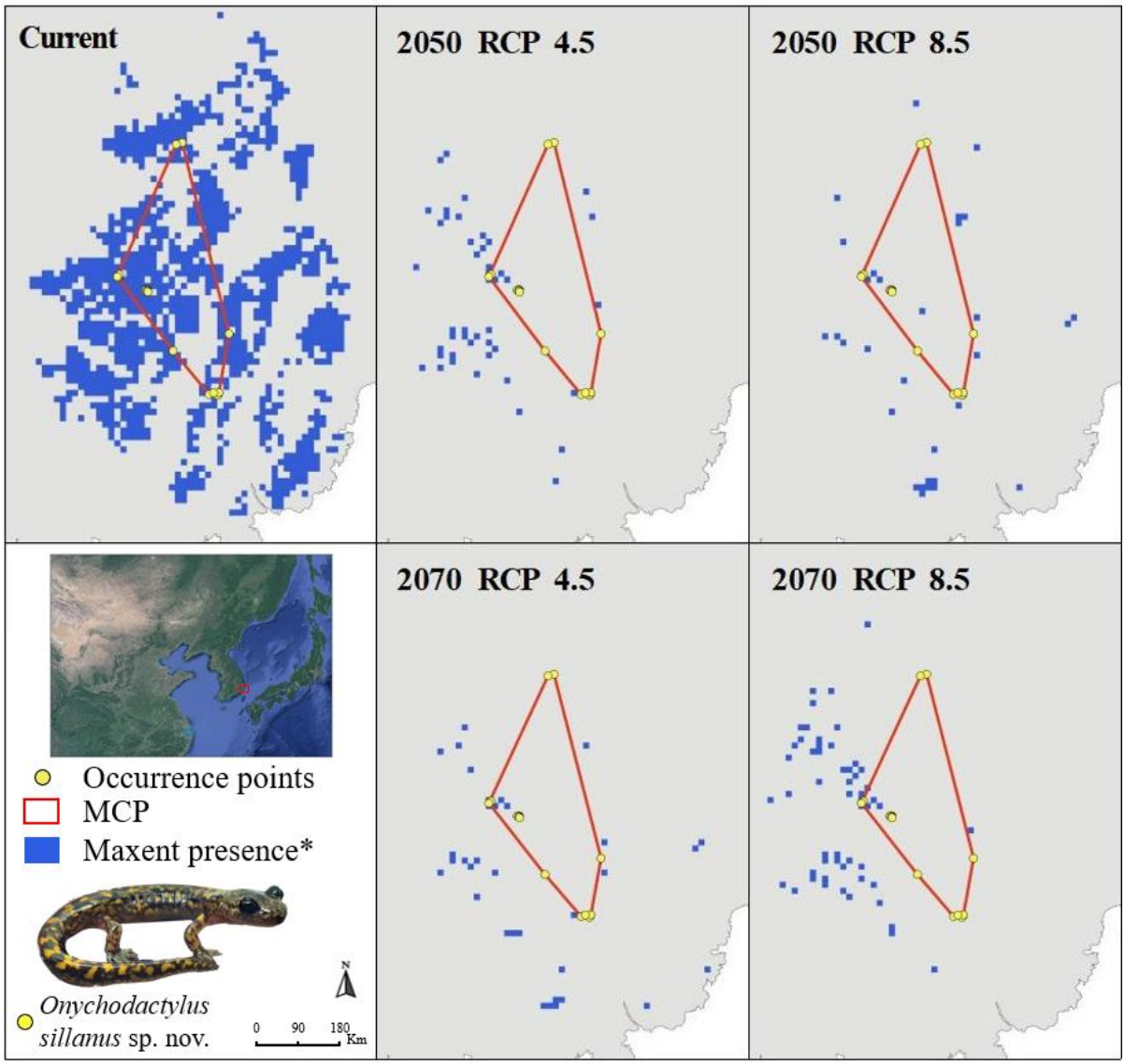

Supplementary Figure S8. Potential impacts of future climate change on the suitable habitat of *Onychodactylus sillanus* sp. nov. The ecological niche models projected on to four climate change scenarios under two timeframes all predicted significant and drastic contraction of suitable habitat area. Depending on the scenario and time frame, as much as 97% reduction of suitable habitat area was predicted. *The Maxent ranges is binary encoded for presence and absence based on the threshold determined in the text.

Conservation assessment. Based on the international database protected planet (https://www.protectedplanet.net/), the habitat suitability of O. sillanus sp. nov. overlaps with several protected area of significance. The species is also present in the five following protected areas, or within its vicinity and most likely to be found in the area: Hoedong Water Source Protection Area (www.protectedplanet.net/555622430), Gyeongnam Yangsan Habuk-myeon 1 Wildlife Protection Area (www.protectedplanet.net/555625924), Gyeongnam Yangsan Habuk-myeon 2 Wildlife Protection Area (www.protectedplanet.net/555625925), Cheong-do Unmunsan Ecosystem and Landscape Conservation Area (www.protectedplanet.net/555558241) and Unmunsan County Park (www.protectedplanet.net/555571343).
The preliminary assessments provided by the *ConR* package put *O. sillanus* sp. nov. in the Endangered category based on B1a and B2a criteria.

Discussion

By describing the species with a focus on conservation we aim at highlighting the general extinction denial surrounding the current 6th mass extinction (Lees et al., 2020). This global problem is also prevalent in the Republic of Korea (Lee & Miller-Rushing, 2014), despite the potential for conservation being currently at its highest (Borzée et al., 2019b). This stems from the availability of monetary resources following the rapid development of the nation (Kim, 2005) coupled with the general interest for a betterment of conservation activities in the nation when supported by popular support, as seen with Bottlenose dolphins (Kim & Tatar, 2018) and Asiatic black bears (Andersen et al., 2021). However, a high number of extinctions is foreseeable in the near future (NIBR, 2014), with numerous species in need of urgent actions (Borzée et al., 2018; Hong et al., 2007; Kim et al., 2013; Zöckler et al., 2010). *Onychodactylus sillanus* sp. nov. is currently the source of legal actions and citizen actions to protect its habitat from urbanisation and groundwater development (Choi, 2020a, 2020b; Kim, 2021). Action plan for amphibians generally include a list of main threats and actions to counter these threats (Wren et al., 2015), and can originate from both governmental, non-governmental or citizen agencies. Examples of conservation action plans for salamanders include the recovery plans for Sonora tiger salamander (*Ambystoma tigrinum stebbinsi*; U. S. Fish and Wildlife Service, 2002) or Dusky salamanders (*Desmognathus* sp.; Markle et al., 2013) where all known threats, and resolutions are described.

The inability to test for reproductive isolation of the two species does not affect the species status of the species as hybridisation is now known to be common between species (Arntzen et al., 2021; Myers, 2021; Rancilhac et al., 2021). However, additional nuclear markers could show a discordance between mitochondrial and nuclear DNA. Here, isolation between the two clades was reached 6 million years ago due to geological events, a timeline well within the average "lifetime" of a species (1 to 10 million years; Raup, 1978). In this regard, we can assume that the two species likely went through the process of allopatric speciation as a result of the Yangsan fault, similarly to other hynobiid species (Borzée and Min, 2021). *Onychodactylus sillanus* sp. nov. is therefore an independent evolutionary and

conservation unit, in dire need of conservation actions to avoid extinction within three generation times because of anthropogenic climate change and other anthropogenic threats.

Our results further agree with the earlier studies (Poyarkov et al., 2012; Suk et al., 2018) in recognizing significant diversity within *O. koreanus* sensu stricto, however without a clear geographic structuring (Figure 1). Our study also confirms the earlier results of Suk et al. (2018) on the putative candidate species status of the *Onychodactylus* sp. A lineage from Gangwon Province, R. Korea. Further integrative studies and analyses of its distribution are urgently needed to assess its taxonomic and conservation status.

The habitat suitability of *Onychodactylus sillanus* sp. nov. predicted by landscape analyses is more appropriately interpreted as identifying areas with potentially suitable environmental conditions instead of delineating the actual range boundaries between the candidate clade and *O. koreanus* (Pearson et al., 2007). This is reflected in our ENM, which predicted areas of high habitat suitability far outside the known range of the candidate clade. In this regard, the actual range of the candidate clade could be more restricted than the area of current suitable habitat estimated from the Maxent binary presence. This further highlights the need for policies that consider biodiversity protection and the designation of protected areas that correspond to biodiverse areas and address the current bias towards low-human density but biodiversity poor areas (Choe et al., 2018; Shin, 2009).

References

Aiello-Lammens ME, Boria RA, Radosavljevic A, Vilela B, Anderson RP. 2015. spThin: an R package for spatial thinning of species occurrence records for use in ecological niche models. *Ecography*, **38**(5): 541–545.

Allouche O, Tsoar A, Kadmon R. 2006. Assessing the accuracy of species distribution models: prevalence, kappa and the true skill statistic (TSS). *Journal of Applied Ecology*, **43**(6): 1223–1232.

Amatulli G, Domisch S, Tuanmu MN, Parmentier B, Ranipeta A, Malczyk J, et al. 2018. A suite of global, cross-scale topographic variables for environmental and biodiversity modeling. *Scientific Data*, **5**: 180040.

Andersen A, Yi Y, Borzée A, Kim K, Moon K, Kim J, et al. 2021. Modelling population dynamics and habitat connectivity for a reintroduced ursid population. *Oryx*, in press.

Arntzen JW, Jehle R, Wielstra B. 2021. Genetic and morphological data demonstrate hybridization and backcrossing in a pair of salamanders at the far end of the speciation continuum. *Evolutionary Applications*, **14**(12): 2784–2793.

Bae HG, Suk HY. 2015. Population genetic structure and colonization history of short ninespine sticklebacks (*Pungitius kaibarae*). *Ecology and Evolution*, **5**(15): 3075–3089.

Bolam FC, Mair L, Angelico M, Brooks TM, Burgman M, Hermes C, et al. 2021. How many bird and mammal extinctions has recent conservation action prevented?. *Conservation Letters*, **14**(1): e12762.

Borzée A. 2020. Recommendations for IUCN Red List conservation status of the "*Dryophytes immaculatus* group" in North East Asia. *Diversity*, **12**(9): 336.

Borzée A, Andersen D, Groffen J, Kim HT, Bae Y, Jang Y. 2019a. Climate change-based models predict range shifts in the distribution of the only Asian plethodontid salamander: *Karsenia koreana*. *Scientific Reports*, **9**(1): 11838.

Borzée A, Andersen D, Jang Y. 2018. Population trend inferred from aural surveys for calling anurans in Korea. *PeerJ*, **6**: e5568.

Borzée A, Litvinchuk SN, Ri K, Andersen D, Nam TY, Jon GH, et al. 2021. Update on distribution and conservation status of amphibians in the Democratic People's Republic of

Korea: conclusions based on field surveys, environmental modelling, molecular analyses and call properties. *Animals*, **11**(7): 2057.
Borzée A, Min MS. 2021. Disentangling the impacts of speciation, sympatry and the island effect on the morphology of seven *Hynobius* sp. salamanders. *Animals*, **11**(1): 187.
Borzée A, Struecker MY, Yi Y, Kim D, Kim H. 2019b. Time for Korean wildlife conservation. *Science*, **363**(6432): 1161–1162.
Brodie JF, Aslan CE, Rogers HS, Redford KH, Maron JL, Bronstein JL, et al. 2014. Secondary extinctions of biodiversity. *Trends in Ecology & Evolution*, **29**(12): 664–672.
Chen MY, Mao RL, Liang D, Kuro-o M, Zeng XM, Zhang P. 2015. A reinvestigation of phylogeny and divergence times of Hynobiidae (Amphibia, Caudata) based on 29 nuclear genes. *Molecular Phylogenetics and Evolution*, **83**: 1–6.
Choe H, Thorne JH, Huber PR, Lee D, Quinn JF. 2018. Assessing shortfalls and complementary conservation areas for national plant biodiversity in South Korea. *PLoS One*, **13**(2): e0190754.
Choi H. 2020a (2020-10-12). A unique salamander in the world, found in Mt. Geumjeong [in Korean]. in Busan and Gyeongnam representative broadcasting KNN, http://www.knn.co.kr/215705. (in Korean).
Choi H. 2020b (2020-10-14). A world-unique salamander doesn't have the right to be protected? [in Korean]. in Busan and Gyeongnam representative broadcasting KNN, http://www.knn.co.kr/215854. (in Korean).
Cop21. 2015. Paris Climate Agreement. Paris, France: United Nations.
Dauby G. 2020 (2020-05-18). ConR: computation of parameters used in preliminary assessment of conservation status. Version 1.3.0, https://CRAN.R-project.org/package=ConR.
Fick SE, Hijmans RJ. 2017. WorldClim 2: new 1-km spatial resolution climate surfaces for global land areas. *International Journal of Climatology*, **37**(12): 4302–4315.
Glor RE, Warren DL. 2011. Testing ecological explanations for biogeographic boundaries. *Evolution*, **65**(3): 673–683.
Hall TA. 1999. BioEdit: a user-friendly biological sequence alignment editor and analysis program for Windows 95/98/NT. *Nucleic Acids Symposium Series*, **41**: 95–98.
Hayek LAC, Heyer WR, Gascon C. 2001. Frog morphometrics: a cautionary tale. *Alytes*, **18**(3–4): 153–177.
Hijmans RJ, Phillips S, Leathwick J, Elith J. 2021 (2021-10-11). dismo: species distribution modeling. Version 1.3-5, https://CRAN.R-project.org/package=dismo.
Hoang DT, Chernomor O, von Haeseler A, Minh BQ, Vinh LS. 2018. UFBoot2: improving the ultrafast bootstrap approximation. *Molecular Biology and Evolution*, **35**(2): 518–522.
Hong JS, Yamashita H, Sato SI. 2007. The Saemangeum Reclamation Project in South Korea threatens to extinguish an unique mollusk, ectosymbiotic bivalve species attached to the shell of *Lingula anatina*. *Plankton and Benthos Research*, **2**(1): 70–75.
Hong NR. 2017. Habitat environmental characteristics of Korean clawed salamander (*Onychodactylus koreanus*) at Mt. Baegun in Guangyang, Jeonnam province. Master thesis, Seoul national University, Seoul.
Huelsenbeck JP, Ronquist F. 2001. MRBAYES: bayesian inference of phylogenetic trees. *Bioinformatics*, **17**(8): 754–755.
Hurney CA, Babcock SK, Shook DR, Pelletier TM, Turner SD, Maturo J, et al. 2015. Normal table of embryonic development in the four-toed salamander, Hemidactylium scutatum. *Mechanisms of Development*, **136**: 99–110.
IPCC. 2014. Climate change 2014: synthesis report. Washington: U.S. Global Change Research Program.

IPCC. 2018. Summary for policymakers. *In*: Masson-Delmotte V, Zhai P, Pörtner HO, Roberts D, Skea J, Shukla PR, et al. Global Warming of 1.5°C. Geneva, Switzerland: World Meteorological Organization, 32.
IUCN. 1989. IUCN policy statement on research involving species at risk of extinction. Editon. Gland, Switzerland: International Union for the Conservation of Nature.
IUCN. 2012. IUCN Red List categories and criteria, version 3.1. 2nd ed. Gland: IUCN.
Jane SF, Hansen GJA, Kraemer BM, Leavitt PR, Mincer JL, North RL, et al. 2021. Widespread deoxygenation of temperate lakes. *Nature*, **594**(7861): 66–70.
Katoh K, Misawa K, Kuma KI, Miyata T. 2002. MAFFT: a novel method for rapid multiple sequence alignment based on fast Fourier transform. *Nucleic Acids Research*, **30**(14): 3059–3066.
Kim D, Conway KW, Jeon HB, Kwon YS, Won YJ. 2013. High genetic diversity within the morphologically conservative dwarf loach, *Kichulchoia brevifasciata* (Teleostei: Cobitidae), an endangered freshwater fish from South Korea. *Conservation Genetics*, **14**(4): 757–769.
Kim HT, Kim H, Jeon G, Kim D. 2019. Arrow guide of amphibians and reptiles. Seoul, Republic of Korea: Econature.
Kim HW, Yoon S, Kim M, Shin M, Yoon H, Kim K. 2021. EcoBank: a flexible database platform for sharing ecological data. *Biodiversity Data Journal*, **9**: e61866.
Kim K. 2021 (2021-11-05). Environmental groups plead for retraction on the plan to develop groundwater in the Sasong area of Yangsan [in Korean]. in Gyeongnam Ilbo, http://www.ksilbo.co.kr/news/articleView.html?idxno=917678. (in Korean).
Kim S, Tatar B. 2018. Dolphin liberation in Korea: is it beneficial for conservation?. *Coastal Management*, **46**(3): 222–234.
Kumar S, Stecher G, Li M, Knyaz C, Tamura K. 2018. MEGA X: molecular evolutionary genetics analysis across computing platforms. *Molecular Biology and Evolution*, **35**(6): 1547–1549.
Kuzmin SL. 1995. The Clawed Salamanders of Asia: Genus *Onychodactylus*. Magdeburg, Germany: Westarp Wissenschaften.
Kyung JB. 2010. Paleoseismological study and evaluation of maximum earthquake magnitude along the Yangsan and Ulsan fault zones in the southeastern part of Korea. *Geophysics and Geophysical Exploration*, **13**(3): 187–197.
Lanfear R, Frandsen PB, Wright AM, Senfeld T, Calcott B. 2017. PartitionFinder 2: new methods for selecting partitioned models of evolution for molecular and morphological phylogenetic analyses. *Molecular Biology and Evolution*, **34**(3): 772–773.
Leaché AD, Reeder TW. 2002. Molecular systematics of the eastern fence lizard (*Sceloporus undulatus*): a comparison of parsimony, likelihood, and Bayesian approaches. *Systematic Biology*, **51**(1): 44–68.
Lee JH, Park D. 2016. The encyclopedia of Korean amphibians. Seoul, Republic of Korea: Checklist of Organisms in Korea 17.
Lee SD, Miller-Rushing AJ. 2014. Degradation, urbanization, and restoration: a review of the challenges and future of conservation on the Korean Peninsula. *Biological Conservation*, **176**: 262–276.
Lees AC, Attwood S, Barlow J, Phalan B. 2020. Biodiversity scientists must fight the creeping rise of extinction denial. *Nature Ecology & Evolution*, **4**(11): 1440–1443.
Librado P, Rozas J. 2009. DnaSP v5: a software for comprehensive analysis of DNA polymorphism data. *Bioinformatics*, **25**(11): 1451–1452.
Lindenmayer DB, Fischer J. 2013. Habitat Fragmentation and Landscape Change: an Ecological and Conservation Synthesis. Washington, USA: Island Press.

Lleonart J, Salat J, Torres GJ. 2000. Removing allometric effects of body size in morphological analysis. *Journal of Theoretical Biology*, **205**(1): 85–93.
Mace GM, Collar NJ, Gaston KJ, Hilton-Taylor C, Akçakaya HR, Leader-Williams N, et al. 2008. Quantification of extinction risk: IUCN's system for classifying threatened species. *Conservation Biology*, **22**(6): 1424–1442.
Maes D, Isaac NJB, Harrower CA, Collen B, van Strien AJ, Roy DB. 2015. The use of opportunistic data for IUCN Red List assessments. *Biological Journal of the Linnean Society*, **115**(3): 690–706.
Mahler BJ, Bourgeais R. 2013. Dissolved oxygen fluctuations in karst spring flow and implications for endemic species: Barton Springs, Edwards aquifer, Texas, USA. *Journal of Hydrology*, **505**: 291–298.
Manne LL, Pimm SL. 2001. Beyond eight forms of rarity: which species are threatened and which will be next?. *Animal Conservation*, **4**(3): 221–229.
Markle TM, Yagi AR, Green DM. 2013. EXECUTIVE SUMMARY – Recovery strategy for the allegheny mountain dusky salamander (*Desmognathus ochrophaeus*) and the northern dusky salamander (*Desmognathus fuscus*) in Ontario. Peterborough, Ontario: Ontario Ministry of Natural Resources.
Maslova IV, Portnyagina EY, Sokolova DA, Vorobieva PA, Akulenko MV, Portnyagin AS, et al. 2018. Distribution of rare and endangered amphibians and reptiles in Primorsky Krai (Far East, Russia). *Nature Conservation Research*, **3**(Suppl. 1): 61–72.
Matsui M, Yoshikawa N, Tominaga A, Sato T, Takenaka S, Tanabe S, et al. 2008. Phylogenetic relationships of two *Salamandrella* species as revealed by mitochondrial DNA and allozyme variation (Amphibia: Caudata: Hynobiidae). *Molecular Phylogenetics and Evolution*, **48**(1): 84–93.
Misawa Y. 1989. The method of counting costal grooves. *In*: Matsui M, Hikida T, Gorris RC. Current Herpetology in East Asia. Kyoto, Japan: Hepetological Society of Japan, 129–134.
Monroe MJ, Butchart SHM, Mooers AO, Bokma F. 2019. The dynamics underlying avian extinction trajectories forecast a wave of extinctions. *Biology Letters*, **15**(12): 20190633.
Mundaca L, Ürge-Vorsatz D, Wilson C. 2019. Demand-side approaches for limiting global warming to 1.5 °C. *Energy Efficiency*, **12**(2): 343–362.
Muscarella R, Galante PJ, Soley-Guardia M, Boria RA, Kass JM, Uriarte M, et al. 2014. ENMeval: an R package for conducting spatially independent evaluations and estimating optimal model complexity for Maxent ecological niche models. *Methods in Ecology and Evolution*, **5**(11): 1198–1205.
Myers EA. 2021. Genome-wide data reveal extensive gene flow during the diversification of the western rattlesnakes (Viperidae: Crotalinae: *Crotalus*). *Molecular Phylogenetics and Evolution*, **165**: 107313.
Kim NC. 2005. Ecological restoration and revegetation works in Korea. *Landscape and Ecological Engineering*, **1**(1): 77–83.
Neam K, Borzée A. 2021. IUCN Red List update!. *FrogLog*, **28**(1): 122.
Nishikawa K, Matsui M, Tanabe S, Sato SI. 2007. Morphological and allozymic variation in *Hynobius boulengeri* and *H. stejnegeri* (Amphibia: Urodela: Hynobiidae). *Zoological Science*, **24**(7): 752–766.
Osorio-Olvera L, Lira-Noriega A, Soberón J, Peterson AT, Falconi M, Contreras-Díaz RG, et al. 2020. NTBOX: an R package with graphical user interface for modelling and evaluating multidimensional ecological niches. *Methods in Ecology and Evolution*, **11**(10): 1199–1206.
Park D. 2005. The first observation of breeding of the long-tailed clawed salamander, *Onychodactylus fischeri*, in the field. *Current Herpetology*, **24**(1): 7–12.

Pearson RG, Raxworthy CJ, Nakamura M, Peterson AT. 2007. Predicting species distributions from small numbers of occurrence records: a test case using cryptic geckos in Madagascar. *Journal of Biogeography*, **34**(1): 102–117.
Poyarkov Jr NA, Che J, Min MS, Kuro-o M, Yan F, Li C, et al. 2012. Review of the systematics, morphology and distribution of Asian Clawed Salamanders, genus *Onychodactylus* (Amphibia, Caudata: Hynobiidae), with the description of four new species. *Zootaxa*, **3465**(1): 1–106.
Pyron RA, Burbrink FT. 2009. Lineage diversification in a widespread species: roles for niche divergence and conservatism in the common kingsnake, *Lampropeltis getula*. *Molecular Ecology*, **18**(16): 3443–3457.
R Core Team 2020. R: A language and environment for statistical computing. R Foundation for Statistical Computing, Vienna, Austria. URL https://www.R-project.org/.
Rambaut A, Drummond AJ. 2013. Tracer 1.6. Edinburgh, UK: University of Edinburgh.
Rancilhac L, Irisarri I, Angelini C, Arntzen JW, Babik W, Bossuyt F, et al. 2021. Phylotranscriptomic evidence for pervasive ancient hybridization among Old World salamanders. *Molecular Phylogenetics and Evolution*, **155**: 106967.
Raup DM. 1978. Cohort analysis of generic survivorship. *Paleobiology*, **4**(1): 1–15.
Régnier C, Achaz G, Lambert A, Cowie RH, Bouchet P, Fontaine B. 2015. Mass extinction in poorly known taxa. *Proceedings of the National Academy of Sciences of the United States of America*, **112**(25): 7761–7766.
Rissler LJ, Apodaca JJ. 2007. Adding more ecology into species delimitation: ecological niche models and phylogeography help define cryptic species in the black salamander (*Aneides flavipunctatus*). *Systematic Biology*, **56**(6): 924–942.
Rix MG, Huey JA, Main BY, Waldock JM, Harrison SE, Comer S, et al. 2017. Where have all the spiders gone? The decline of a poorly known invertebrate fauna in the agricultural and arid zones of southern Australia. *Austral Entomology*, **56**(1): 14–22.
Ronquist F, Huelsenbeck JP. 2003. MrBayes 3: bayesian phylogenetic inference under mixed models. *Bioinformatics*, **19**(12): 1572–1574.
Sato I. 1943. The tailed batrachians of Japan. *Copeia*, **1943**: 1–520.
Shin W. 2009. Korea's Protected Areas: Evaluating the Effectiveness of South Korea's Protected Areas System. Seoul, Republic of Korea: Korean National Parks Service.
Shin Y, Jang Y, Allain SJR, Borzée A. 2020a. Catalogue of herpetological specimens of the Ewha Womans University Natural History Museum (EWNHM), Republic of Korea. *ZooKeys*, **965**: 103–139.
Shin Y, Jeong D, Borzée A. 2020b. Mass displacement of Korean clawed salamanders (*Onychodactylus koreanus*) and the threat of road-kill. *Herpetological Bulletin*, **151**: 28–31.
Shin Y, Messenger KR, Koo KS, Lee SC, Hou M, Borzée A. 2021a. How threatened is *Scincella huanrenensis*? An update on threats and trends. *Conservation*, **1**(1): 58–72.
Shin Y, Min MS, Borzée A. 2021b. Driven to the edge: species distribution modeling of a Clawed Salamander (Hynobiidae: *Onychodactylus koreanus*) predicts range shifts and drastic decrease of suitable habitats in response to climate change. *Ecology and Evolution*, **11**(21): 14669–14688.
Shu GC, Gong YZ, Xie F, Wu NC, Li C. 2017. Effects of long-term preservation on amphibian body conditions: implications for historical morphological research. *PeerJ*, **5**: e3805.
Smirina EM. 1994. Age determination and longevity in amphibians. *Gerontology*, **40**(2–4): 133–146.
Suh MI, Lee BY, Kim ST, Park CH, Oh HK. 2014. Korean Red List of Threatened Species. 2nd ed. Incheon, Republic of Korea: National Institute of Biological Resources.

Suk HY, Lee MY, Bae HG, Lee SJ, Poyarkov Jr N, Lee H, et al. 2018. Phylogenetic structure and ancestry of Korean clawed salamander, *Onychodactylus koreanus* (Caudata: Hynobiidae). *Mitochondrial DNA Part A*, **29**(4): 650–658.
Tedesco PA, Bigorne R, Bogan AE, Giam X, Jézéquel C, Hugueny B. 2014. Estimating how many undescribed species have gone extinct. *Conservation Biology*, **28**(5): 1360–1370.
Tuanmu MN, Jetz W. 2014. A global 1-km consensus land-cover product for biodiversity and ecosystem modelling. *Global Ecology and Biogeography*, **23**(9): 1031–1045.
U.S. Fish and Wildlife Service. 2002. Sonora Tiger Salamander (*Ambystoma tigrinum stebbinsi*) Recovery Plan. Phoenix, Arizona: U.S. Fish and Wildlife Service.
Warren DL, Matzke NJ, Cardillo M, Baumgartner JB, Beaumont LJ, Turelli M, et al. 2021. ENMTools 1.0: an R package for comparative ecological biogeography. *Ecography*, **44**(4): 504–511.
Weisrock DW, Macey JR, Matsui M, Mulcahy DG. 2013. Molecular phylogenetic reconstruction of the endemic Asian salamander family Hynobiidae (Amphibia, Caudata). *Zootaxa*, **3626**(1): 77–93.
Wren S, Angulo A, Meredith H, Kielgast J, Dos Santos M, Bishop P. 2015. Amphibian conservation action plan. https://www.iucn-amphibians.org/resources/acap/.
Xu Y, Zhou BT, Wu J, Han ZY, Zhang YX, Wu J. 2017. Asian climate change under 1.5–4 ℃ warming targets. *Advances in Climate Change Research*, **8**(2): 99–107.
Yoshikawa N, Matsui M. 2013. A new salamander of the genus *Onychodactylus* from Tsukuba Mountains, Eastern Honshu, Japan (Amphibia, Caudata, Hynobiidae). *Current Herpetology*, **32**(1): 9–25.
Yoshikawa N, Matsui M. 2014. Two new salamanders of the genus *Onychodactylus* from eastern Honshu, Japan (Amphibia, Caudata, Hynobiidae). *Zootaxa*, **3866**(1): 53–78.
Yoshikawa N, Matsui M. 2022. A new salamander of the genus *Onychodactylus* from central Honshu, Japan (Amphibia, Caudata, Hynobiidae). *Current Herpetology*, **41**(1): 82–100.
Yoshikawa N, Matsui M, Nishikawa K, Kim JB, Kryukov A. 2008. Phylogenetic relationships and biogeography of the Japanese clawed salamander, *Onychodactylus japonicus* (Amphibia: Caudata: Hynobiidae), and its congener inferred from the mitochondrial cytochrome b gene. *Molecular Phylogenetics and Evolution*, **49**(1): 249–259.
Yoshikawa N, Matsui M, Tanabe S, Okayama T. 2013. Description of a new salamander of the genus *Onychodactylus* from Shikoku and Western Honshu, Japan (Amphibia, Caudata, Hynobiidae). *Zootaxa*, **3693**(4): 441–464.
Zhang P, Chen YQ, Zhou H, Liu YF, Wang XL, Papenfuss TJ, et al. 2006. Phylogeny, evolution, and biogeography of Asiatic salamanders (Hynobiidae). *Proceedings of the National Academy of Sciences of the United States of America*, **103**(19): 7360–7365.
Zhang ZX, Mammola S, Liang ZQ, Capinha C, Wei QW, Wu YN, et al. 2020. Future climate change will severely reduce habitat suitability of the Critically Endangered Chinese giant salamander. *Freshwater Biology*, **65**(5): 971–980.
Zheng YC, Peng R, Kuro-o M, Zeng XM. 2011. Exploring patterns and extent of bias in estimating divergence time from mitochondrial DNA sequence data in a particular lineage: a case study of salamanders (Order Caudata). *Molecular Biology and Evolution*, **28**(9): 2521–2535.
Zheng YC, Peng R, Murphy RW, Kuro-o M, Hu LJ, Zeng XM. 2012. Matrilineal genealogy of *Hynobius* (Caudata: Hynobiidae) and a temporal perspective on varying levels of diversity among lineages of salamanders on the Japanese Islands. *Asian Herpetological Research*, **3**(4): 288–302.

Zöckler C, Syroechkovskiy EE, Atkinson PW. 2010. Rapid and continued population decline in the Spoon-billed Sandpiper *Eurynorhynchus pygmeus* indicates imminent extinction unless conservation action is taken. *Bird Conservation International*, **20**(2): 95–111.